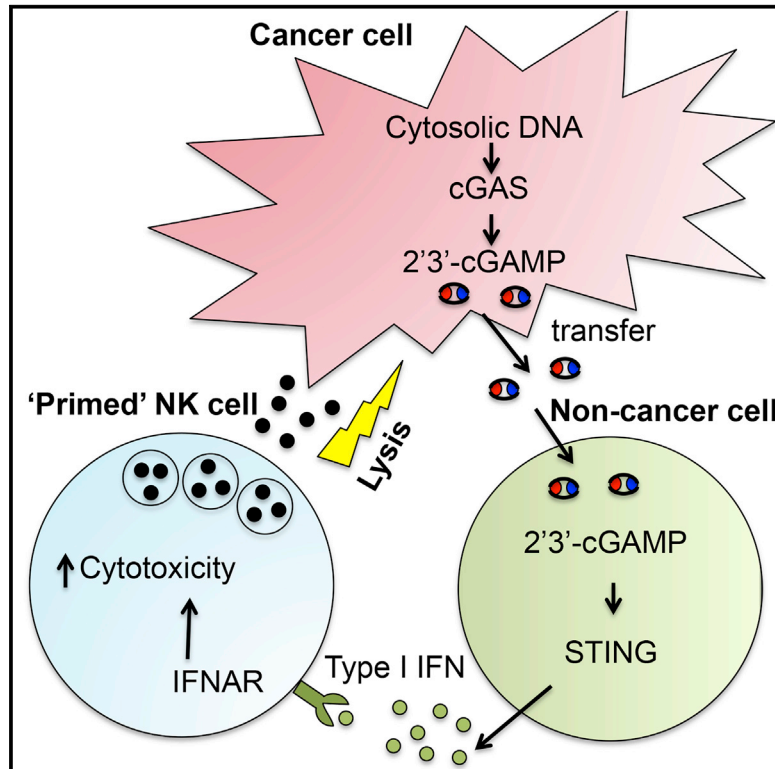


Immunity

Tumor-Derived cGAMP Triggers a STING-Mediated Interferon Response in Non-tumor Cells to Activate the NK Cell Response

Graphical Abstract



Authors

Assaf Marcus, Amy J. Mao,
Monisha Lensink-Vasan,
LeeAnn Wang, Russell E. Vance,
David H. Raulet

Correspondence

rvance@berkeley.edu (R.E.V.),
raulet@berkeley.edu (D.H.R.)

In Brief

Marcus et al. find that cGAMP produced by tumor cells triggers the activation of the STING pathway in immune cells within the tumor microenvironment. This leads to interferon production by these cells, which in turn activates NK cell anti-tumor immunity.

Highlights

- *Sting*^{-/-} mice, but not *Cgas*^{-/-} mice, fail to mount optimal NK cell anti-tumor responses
- *Cgas*^{-/-} tumor cells are defective in inducing anti-tumor responses by NK cells
- cGAS is constitutively active in tumor cells but not in untransformed cells
- cGAMP is transferred from tumor cells to other cells in the TME to activate STING



Tumor-Derived cGAMP Triggers a STING-Mediated Interferon Response in Non-tumor Cells to Activate the NK Cell Response

Assaf Marcus,¹ Amy J. Mao,¹ Monisha Lensink-Vasan,¹ LeeAnn Wang,¹ Russell E. Vance,^{1,2,3,4,*} and David H. Raulet^{1,2,3,5,*}

¹Division of Immunology and Pathogenesis, Department of Molecular and Cell Biology, University of California, Berkeley, Berkeley, CA 94720, USA

²Cancer Research Laboratory, University of California, Berkeley, Berkeley, CA 94720, USA

³Immunotherapeutics and Vaccine Research Initiative, University of California, Berkeley, Berkeley, CA 94720, USA

⁴Howard Hughes Medical Institute, University of California, Berkeley, Berkeley, CA 94720, USA

⁵Lead Contact

*Correspondence: rvance@berkeley.edu (R.E.V.), raulet@berkeley.edu (D.H.R.)

<https://doi.org/10.1016/j.immuni.2018.09.016>

SUMMARY

Detection of cytosolic DNA by the enzyme cGAS triggers the production of cGAMP, a second messenger that binds and activates the adaptor protein STING, which leads to interferon (IFN) production. Here, we found that *in vivo* natural killer (NK) cell killing of tumor cells, but not of normal cells, depends on STING expression in non-tumor cells. Experiments using transplantable tumor models in STING- and cGAS-deficient mice revealed that cGAS expression by tumor cells was critical for tumor rejection by NK cells. In contrast, cGAS expression by host cells was dispensable, suggesting that tumor-derived cGAMP is transferred to non-tumor cells, where it activates STING. cGAMP administration triggered STING activation and IFN- β production in myeloid cells and B cells but not NK cells. Our results reveal that the anti-tumor response of NK cells critically depends on the cytosolic DNA sensing pathway, similar to its role in defense against pathogens, and identify tumor-derived cGAMP as a major determinant of tumor immunogenicity with implications for cancer immunotherapy.

INTRODUCTION

Natural killer (NK) cells are cytotoxic lymphocytes that can directly kill infected and transformed cells and shape adaptive immune responses by secreting cytokines. NK cell recognition of target cells is mediated by the balance of signaling conveyed by germline-encoded activating receptors for stress-induced or virus-encoded ligands on target cells (Lanier, 2005; Marcus et al., 2014; Yokoyama and Plougastel, 2003) and inhibitory receptors that engage MHC I molecules (Kärre, 2008).

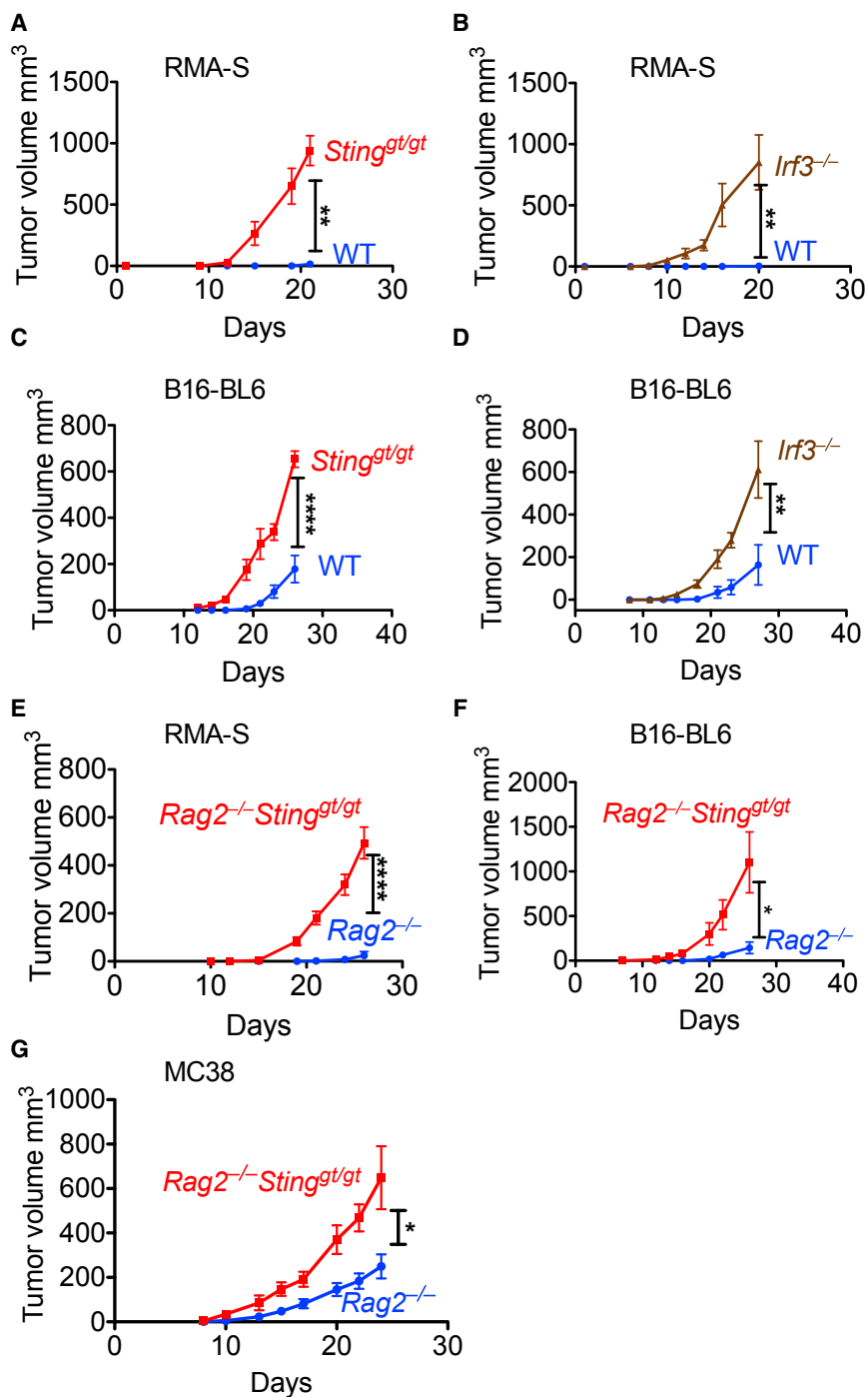
In vivo, NK cells can reject sensitive tumor cells efficiently, but *ex vivo*, resting NK cells obtained from healthy animals or donors often exhibit relatively low cytotoxicity (Diefenbach et al., 2001;

Glas et al., 2000; Raulet, 2004). The mechanisms whereby NK cells acquire strong effector activity *in vivo* against tumor cells are not well defined. Acquisition of strong effector activity ("priming") can be conferred by infections, cytokines (e.g., type I interferon [IFN], interleukin-15 [IL-15], and IL-12), ligands for pattern-recognition receptors (e.g., double-stranded RNA), and vaccination with irradiated tumor cells (Chaix et al., 2008; Diefenbach et al., 2001; Glas et al., 2000; Guia et al., 2008; Mortier et al., 2009). Whether these pathways are relevant in priming NK cell activity in the tumor setting is unclear.

Because IFNs can prime strong effector activity in NK cells, the cGAS-STING pathway is an attractive candidate in considering the activation of NK cells to exert anti-tumor activity. The cGAS-STING pathway mediates cellular immune responses to cytosolic DNA (Chen et al., 2016b; Ishii et al., 2006; Stetson and Medzhitov, 2006). The cGAS enzyme, when bound by cytosolic DNA, catalyzes the synthesis of a cyclic-GMP-AMP dinucleotide called 2'3'-cGAMP (Ablasser et al., 2013a; Diner et al., 2013; Gao et al., 2013b; Wu et al., 2013; Zhang et al., 2013). cGAMP binds and activates the endoplasmic reticulum (ER)-resident adaptor protein STING (stimulator of interferon genes protein) (Ablasser et al., 2013a; Diner et al., 2013; Gao et al., 2013c; Ishikawa et al., 2009; Zhang et al., 2013), which leads to the downstream activation of the transcription factors IFN regulatory factor 3 (IRF3) and nuclear factor κ B (NF- κ B) (Chen et al., 2016b) and the expression of type I IFN, IFN-responsive genes, and various other chemokines and cytokines (e.g., CCL5). The cGAS-STING pathway plays an important role in immune responses to viral infections (Chen et al., 2016b; Ishii et al., 2006; Stetson and Medzhitov, 2006), and emerging evidence in both tumor transfer models and autochthonous models of cancer suggests a role for this pathway in anti-tumor immunity as well (Brzostek-Racine et al., 2011; Gasser and Raulet, 2006a; Härtlova et al., 2015; Lam et al., 2014; Ohkuri et al., 2014; Woo et al., 2014; Zhu et al., 2014).

It has been suggested that DNA leaking from tumor cell nuclei or from dying tumor cells can activate STING in host cells and induce T-cell-mediated anti-tumor responses (Klarquist et al., 2014; Ohkuri et al., 2014; Woo et al., 2014). The model suggests that tumor-derived DNA accesses the cytosol of host antigen-presenting cells (APCs) by some unknown mechanism, whereby it triggers the cGAS-STING pathway and causes IFN production.





IFN causes maturation of APCs and enhances priming of T cells against the tumor. Because STING activation and IFN production can potentially prime strong effector activity in NK cells, the cGAS-STING pathway could be important in the activation of intra-tumoral NK cell responses.

Here, we found that spontaneous *in vivo* NK cell rejection of tumor cells, but not untransformed cells, depends critically on the cGAS-STING pathway. cGAS in tumor cells was active under steady-state conditions and could elicit spontaneous NK cell

Figure 1. *Sting*^{gt/gt} Mice Are Susceptible to Tumors Independently of Effects on T and B Cells

Tumor cells were injected subcutaneously into mice ($n = 4-6$). Tumor growth was assessed by caliper measurements, and statistical significance was assessed by two-way ANOVA. Error bars represent means \pm SEM. Results are representative of two to four independent experiments. Tumors were injected into WT or *Sting*^{gt/gt} mice (A and C), into WT or *Irf3*^{-/-} mice (B and D), or into *Rag2*^{-/-} or *Rag2*^{-/-}*Sting*^{gt/gt} mice (E-G). The mice were injected with the following tumor doses: 2×10^5 RMA-S or RMA cells (A, B, and E), 2×10^4 B16-BL6 cells (C, D, and F), and 10^5 MC38 cells (G).

responses to tumor cells via activation of STING in host cells and subsequent IFN-mediated priming. Our findings provide insight into the mechanisms activating NK cell anti-tumor activity *in vivo* and have implications on the activation of T cells and other immune cells in tumors.

RESULTS

Sting^{gt/gt} Mice Are Susceptible to Tumors Independently of Effects on T and B Cells

STING is important for inducing T cell responses against tumors (Woo et al., 2014). To test whether STING plays a role in anti-tumor responses against tumors that are poorly recognized by T cells, we challenged mice with the TAP2-deficient RMA-S lymphoma and the poorly immunogenic B16-BL6 melanoma. RMA-S lymphoma cells were rejected by wild-type (WT) mice but grew progressively in STING-deficient (*Sting*^{gt/gt}) mice (Figure 1A). Rejection of RMA-S cells was also impaired in mice deficient in IRF3, which acts downstream of STING (Figure 1B). B16-BL6 melanoma tumors also grew more rapidly in *Sting*^{gt/gt} mice and *Irf3*^{-/-} mice than in WT mice (Figures 1C and 1D). To rule out a contribution of T cells or B cells to these anti-tumor responses, we bred *Sting*^{gt/gt} mice

with *Rag2*^{-/-} mice, which lack T and B cells. *Rag2*^{-/-}*Sting*^{gt/gt} mice were significantly more susceptible to RMA-S and B16-BL6 tumor challenge than *Rag2*^{-/-} mice (Figures 1E and 1F).

In response to other transplanted tumors, T cells play an important role, but if the cells are NK sensitive, NK cells can also participate in rejection. For example, T cells play an important role in rejecting the MC38 colon carcinoma, but these cells are also NK sensitive as a result of the expression of ligands for NKG2D and other activating receptors on NK cells. In order to circumvent

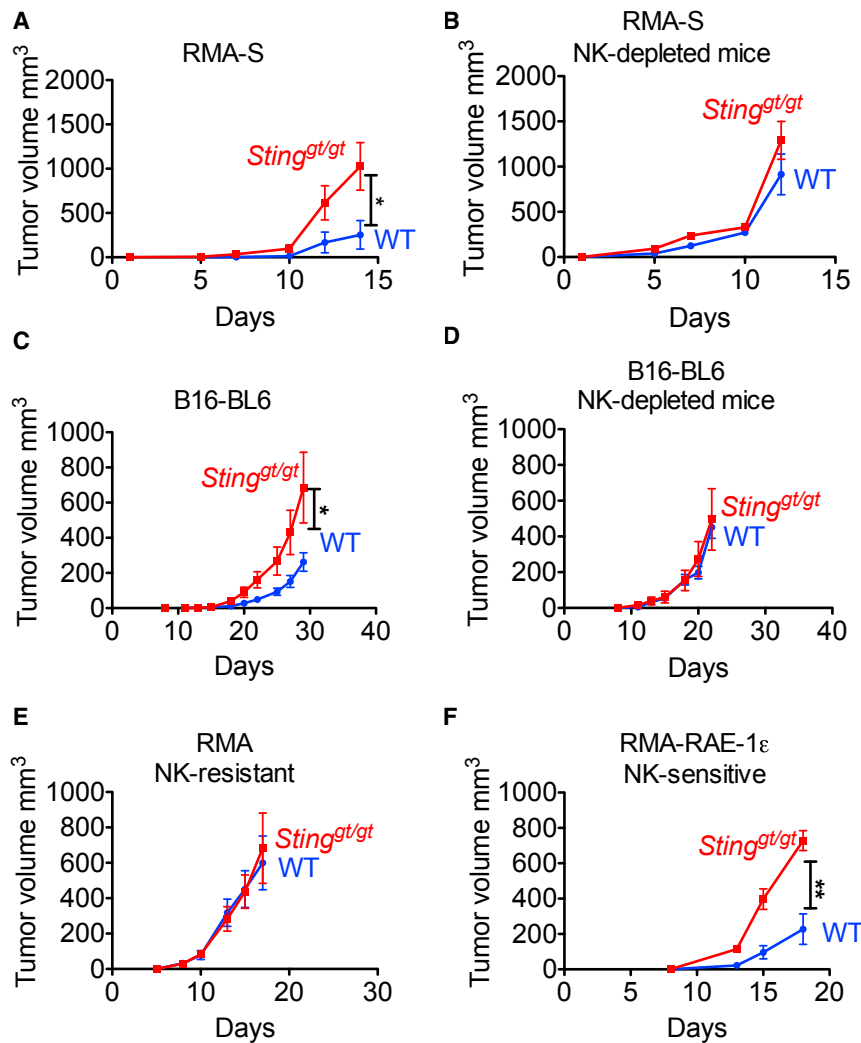


Figure 2. STING Induces NK-Cell-Mediated Anti-tumor Responses

Tumor cells were injected subcutaneously into mice ($n = 4-6$). Tumor growth was assessed by caliper measurements, and statistical significance was assessed by two-way ANOVA. Error bars represent means \pm SEM. Results are representative of two to four independent experiments. In some groups (B and D), NK cells were depleted with PK136 antibody. Tumor cells were injected into WT or *Sting*^{gt/gt} mice. The mice were injected with the following tumor doses: 2×10^5 RMA-S (A and B), 2×10^4 B16-BL6 cells (C and D), 10^5 RMA cells (E), and 5×10^4 RMA-RAE-1 ϵ cells (F).

Despite expression of MHC I, RMA cells are rendered NK sensitive when transduced with an NK-activating ligand, RAE-1 ϵ , a ligand for the NKG2D receptor (Diefenbach et al., 2001). Notably, rejection of RMA-RAE-1 ϵ cells was also dependent on host STING expression (Figure 2F). Therefore, STING is required for the rejection of tumor cells that are sensitive to NK cells as a result of MHC I deficiency or expression of activating ligands. These findings suggest a role for STING against many tumor types, given that NKG2D ligand expression and NK sensitivity are common features of tumors (Raulet et al., 2013).

***Sting*^{gt/gt} Mice Have Functional NK Cells and Are Capable of Rejecting MHC-I-Deficient Bone Marrow Grafts**

We asked whether STING is required for the normal development of NK cells. WT

and *Sting*^{gt/gt} mice contained comparable numbers of splenic NK cells and showed similar expression of phenotypic markers such as CD11b, Ly6C, and NKG2D (Figures 3A–3E), suggesting that this is not the case. Moreover, NK cells in *Sting*^{gt/gt} mice responded normally with respect to cytokine induction when stimulated *ex vivo* with plate-bound antibodies against activating receptors NKp46 and NKG2D (Figure 3F). NK cells in *Sting*^{gt/gt} mice were also functional *in vivo* in rejecting bone marrow grafts from MHC-I-deficient *B2m*^{-/-} mice, whereas negative-control NK-cell-deficient NK-DTA mice were unable to reject *B2m*^{-/-} bone marrow cells, as expected (Figure 3G). These data suggest that STING is essential for NK rejection responses against tumor cells *in vivo* but not for *in vivo* rejection of untransformed MHC-I-deficient cells.

STING Induces NK-Cell-Mediated Anti-tumor Responses

Both RMA-S and B16-BL6 are sensitive to NK cells *in vivo*, suggesting that STING can induce NK cell responses. STING-mediated protection against RMA-S and B16-BL6 tumors (Figures 2A and 2C) was abolished by antibody-mediated depletion of NK cells (Figures 2B and 2D). These analyses confirmed that spontaneous STING-mediated protection against RMA-S and B16-BL6 tumors requires NK cells but not T cells or B cells. Furthermore, host STING played no role in tumor growth when tumors were NK insensitive, as in the case of RMA, the major histocompatibility complex I (MHC I)+ counterpart of RMA-S (Figure 2E). Thus, the impact of STING in these responses is mediated through NK cells and not through the cytostatic effects of IFN or some other NK-independent mechanism.

the T cell response and more clearly reveal the NK cell response, we once again employed mice on the *Rag2* background. *Rag2*^{-/-}*Sting*^{gt/gt} mice were significantly more susceptible than *Rag2*^{-/-} mice to challenge with MC38, thereby establishing the relevance of host STING in yet another tumor model (Figure 1G).

Host cGAS Is Dispensable for Tumor Rejection

It has been previously suggested that, via an unknown mechanism, DNA from dying tumor cells accesses the cytosol of host cells, where it triggers the cGAS-STING pathway and the production of IFN, thus inducing T-cell-mediated anti-tumor responses (Klarquist et al., 2014; Ohkuri et al., 2014; Woo et al., 2014). In light

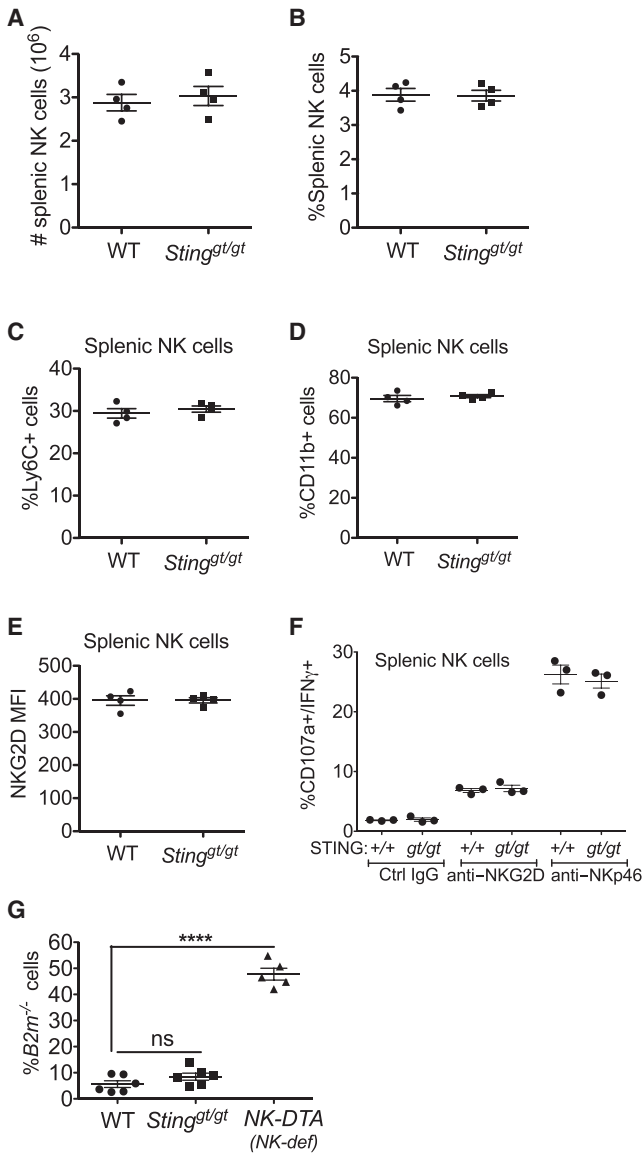


Figure 3. *Sting*^{gt/gt} Mice Have Functional NK Cells and Are Capable of Rejecting MHC-I-Deficient Cells

(A–F) Splenocytes from WT or *Sting*^{gt/gt} mice ($n = 4$) were analyzed by flow cytometry for absolute number (A) or percentage (B) of NK cells, percentages of Ly6C⁺ (C) or CD11b⁺ (D) NK cells, and mean fluorescence intensity of NKG2D staining of NK cells (E). (F) Splenocytes ($n = 3$) were stimulated with plate-bound antibodies (for NKG2D, Nkp46, or control IgG). The percentages of NK cells expressing both CD107a⁺ and IFN- γ ⁺ were assessed by flow cytometry. Statistical significance was assessed with two-tailed t tests, and no significant differences were noted.

(G) Rejection of *B2m*^{-/-} bone marrow cells by WT and *Sting*^{gt/gt} mice but not NK-cell-deficient NK-DTA mice ($n = 5$ or 6). A 50:50 mixture of CFSE-labeled *B2m*^{-/-} and WT bone marrow cells was injected intravenously, and recovery of *B2m*^{-/-} cells was assessed by flow cytometry 3 days later. Results are representative of two to four independent experiments. Statistical significance was assessed by one-way ANOVA with Bonferroni's correction for multiple comparisons.

Error bars represent means \pm SEM.

of the requirement for STING for NK-dependent rejection of tumors, we assessed the requirement for host cGAS, which acts upstream of STING. We used CRISPR/Cas9 technology to generate mice lacking expression of *Cgas* (see STAR Methods). When tested for the anti-tumor NK response, both WT and *Cgas*^{-/-} mice rejected RMA-S and B16-BL6 tumors, demonstrating that host cGAS is not required for these STING-dependent anti-tumor responses (Figures 4A and 4B). As before, *Sting*^{gt/gt} mice tested in parallel were defective in rejecting both of these tumors. As expected, splenocytes from *Cgas*^{-/-} mice failed to respond to stimulation with DNA (Figure 4C) but did respond to stimulation with 2'3'-cGAMP (Figure 4D). *Sting*^{gt/gt} mice, in contrast, failed to respond to stimulation with DNA or with 2'3'-cGAMP (Figures 4C and 4D). In addition, we verified that the numbers and phenotype of NK cells were similar in *Cgas*^{-/-} and WT mice (Figures 4E–4H). Finally, we verified that both *Cgas*^{-/-} mice and *Sting*^{gt/gt} mice exhibited the expected sensitivity to infections with DNA viruses, such as HSV-1 (Figure S1).

Exogenous cGAMP Can Activate NK Cells Extrinsically

The requirement for host STING, but not host cGAS, for anti-tumor NK responses raised the possibility that the 2'3'-cGAMP cyclic dinucleotide necessary to activate STING originates not in host cells but rather in tumor cells. Consistent with the possibility that exogenously supplied cGAMP can activate NK cells, intraperitoneal injections of 2'3'-cGAMP caused NK activation, as shown by increased expression of CD69 and CD137 (4-1BB), and NK cell recruitment to the peritoneum (Figures 5A–5F). NK cell activation and peritoneal recruitment induced by 2'3'-cGAMP were both dependent on STING expression in the recipient mice (Figures 5A–5F). We hypothesized that NK cell activation occurs downstream of STING-induced type I IFN. To test that possibility, we injected 2'3'-cGAMP into WT, *Sting*^{gt/gt}, or *Irfn*^{-/-} mice. NK cell activation, assessed by CD69 activation, was abolished in both *Sting*^{gt/gt} and *Irfn*^{-/-} mice, demonstrating that type I IFN acts downstream of STING to activate NK cells (Figure 5G). We further tested whether type I IFN acts directly on NK cells by transferring *Irfn*^{-/-} splenocytes into congenic CD45.1 mice, allowing for the co-existence of donor and host NK cells in the same animal, and then challenging the mice with 2'3'-cGAMP. Both WT and *Irfn*^{-/-} NK cells were activated, suggesting an indirect effect of IFN on NK cells, but *Irfn*^{-/-} NK cells were not activated as well as WT NK cells, indicating an additional direct effect of IFN on NK cells (Figure 5H). Thus, type I IFN activates NK cells both directly and indirectly.

We stained NK cells for STING expression and found that a subset of them did express STING (Figure 5I), raising the possibility that STING acts intrinsically in NK cells. We therefore tested whether NK-cell-intrinsic STING is necessary for NK cell activation induced by 2'3'-cGAMP. We adoptively transferred splenocytes from *Sting*^{gt/gt} mice into CD45.1 mice and challenged the mice with 2'3'-cGAMP. CD69 expression revealed that 2'3'-cGAMP injections resulted in equivalent activation of WT and *Sting*^{gt/gt} NK cells (Figure 5J), demonstrating that NK-cell-intrinsic STING signaling is dispensable for NK cell activation and that STING must act via other cell type(s).

To address which cells respond to 2'3'-cGAMP, we injected the cyclic dinucleotides directly into RMA-S tumors and then 1 hr later, harvested and incubated the tumors for an additional 5 hr in the presence of Golgi transport inhibitors, allowing for

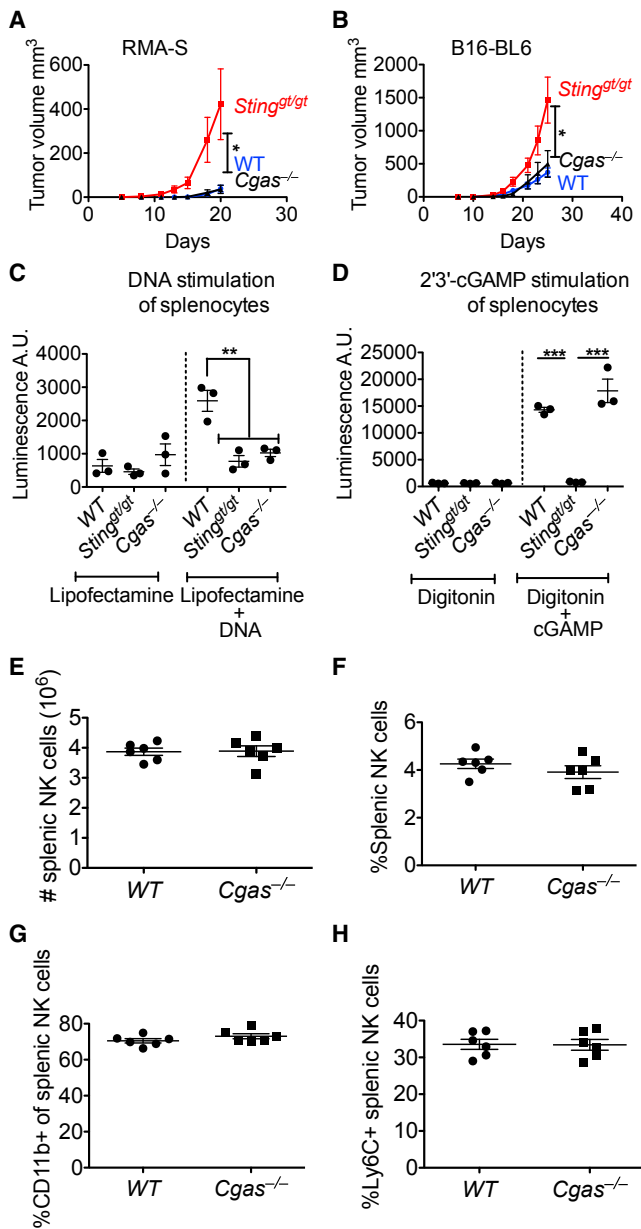


Figure 4. Host cGAS Is Dispensable for Tumor Rejection

(A and B) Tumor cells were injected subcutaneously into WT, *Sting*^{gt/gt}, or *Cgas*^{-/-} mice (n = 4–6). Analysis was as in Figure 1. Results are representative of two independent experiments. Mice were injected with 2×10^5 RMA-S cells (A) or 2×10^4 B16-BL6 cells (B).

(C and D) Splenocytes from WT, *Sting*^{gt/gt}, or *Cgas*^{-/-} mice were transfected with either vaccinia virus dsDNA 70-mer (C) or 2'3'-cGAMP (D), and secreted type I IFN in culture supernatants was measured with an IFN bioassay. Statistical significance was assessed by one-way ANOVA with Bonferroni's correction for multiple comparisons.

(E–H) Splenocytes from WT or *Cgas*^{-/-} mice (n = 6) were analyzed by flow cytometry for the absolute number (E) or percentage (F) of NK cells or the percentages of NK cells expressing CD11b (G) or Ly6C (H). Results are representative of two to four independent experiments. Statistical significance was assessed by two-tailed t tests. Error bars represent means \pm SEM.

cytokines to accumulate. Cells from tumor dissociates were tested for intracellular accumulation of IFN- β by intracellular cytokine staining. IFN- β was detected in CD11b⁺ cells (negative for CD3, CD19, NKp46, and Ly6G), but not in other infiltrating leukocytes such as neutrophils, T cells, or NK cells (Figure 5K), suggesting that these cells play a role when 2'3'-cGAMP is injected into tumors.

B cells were largely absent from these tumors but could play a role in different tumors in response to 2'3'-cGAMP. Indeed, when 2'3'-cGAMP was injected intraperitoneally, intracellular IFN- β was detected in peritoneal B cells when examined *ex vivo*. Together, our results suggest that multiple cell types are capable of responding to 2'3'-cGAMP and that the relevant cells for a given response can be context dependent (Figure 5L).

cGAS Is Specifically Active in Tumor Cells

To test directly whether cGAS in tumor cells is required for tumor rejection mediated by host STING, we used CRISPR/Cas9 technology and two gRNAs concurrently to delete the first exon of *Cgas* in B16-BL6 tumor cells without stably introducing any other marker proteins in the cells. cGAS-deficient B16-BL6 cells failed to respond to DNA stimulation given that they did not increase expression of *Irfn*, *Ccl5*, or *Iffit1* (Figure S2). In the absence of DNA stimulation, WT cells showed significant steady-state expression of cGAS and STING target genes *Ccl5* and the interferon-inducible *Iffit1*, and this expression was significantly reduced in cGAS-deficient B16-BL6 cells, arguing that cGAS is partially active without purposeful induction in the WT tumor cells (Figures 6A and 6B). *Ccl5* and *Iffit1* expression was restored when the mutant tumor cells were transduced with WT cGAS but not enzymatically inactive cGAS (G198A/S199A). Both WT and mutant transduced cGAS were expressed at similar levels to each other but had higher expression than endogenous cGAS. Compared with expression in non-transduced cells, the increased expression of WT cGAS, but not of mutant cGAS, in transduced cells augmented *Ccl5* and *Iffit1* expression. Steady-state activation of the cGAS-STING pathway was also observed in human monocytic cell line THP1, whereby THP1 *TMEM173*^{-/-} cells expressed lower levels of *IFIT1* and *CXCL10* than THP1 WT cells (Figures S3A and S3B). These data suggest that cGAS is active in both tumor cell lines in the absence of exogenous DNA stimulation, which results in low but detectable constitutive expression of IFN-inducible genes. In contrast to the results with the tumor cells, splenocytes, bone marrow cells, lung cells, and liver cells from WT and cGAS-deficient mice expressed similar levels of *Ccl5* and *Iffit1* (Figures 6C and 6D and Figures S3C–S3H). These data indicate that constitutively active cGAS is a distinguishing feature of tumor cells. One possible explanation for the constitutive activation of the cGAS-STING pathway is that it is activated by DNA damage in the tumor cells, as was previously suggested (Ho et al., 2016; Lam et al., 2014; Shen et al., 2015). Indeed, induction of DNA damage in B16 cells by chemotherapy drug ARA-C led to increased cGAS-dependent secretion of type I IFN (Figure S3I).

Expression of cGAS by Tumor Cells Is Crucial for Tumor Rejection

We tested the impact of cGAS expression on tumor rejection *in vivo*. Remarkably, cGAS-deficient tumor cells were not

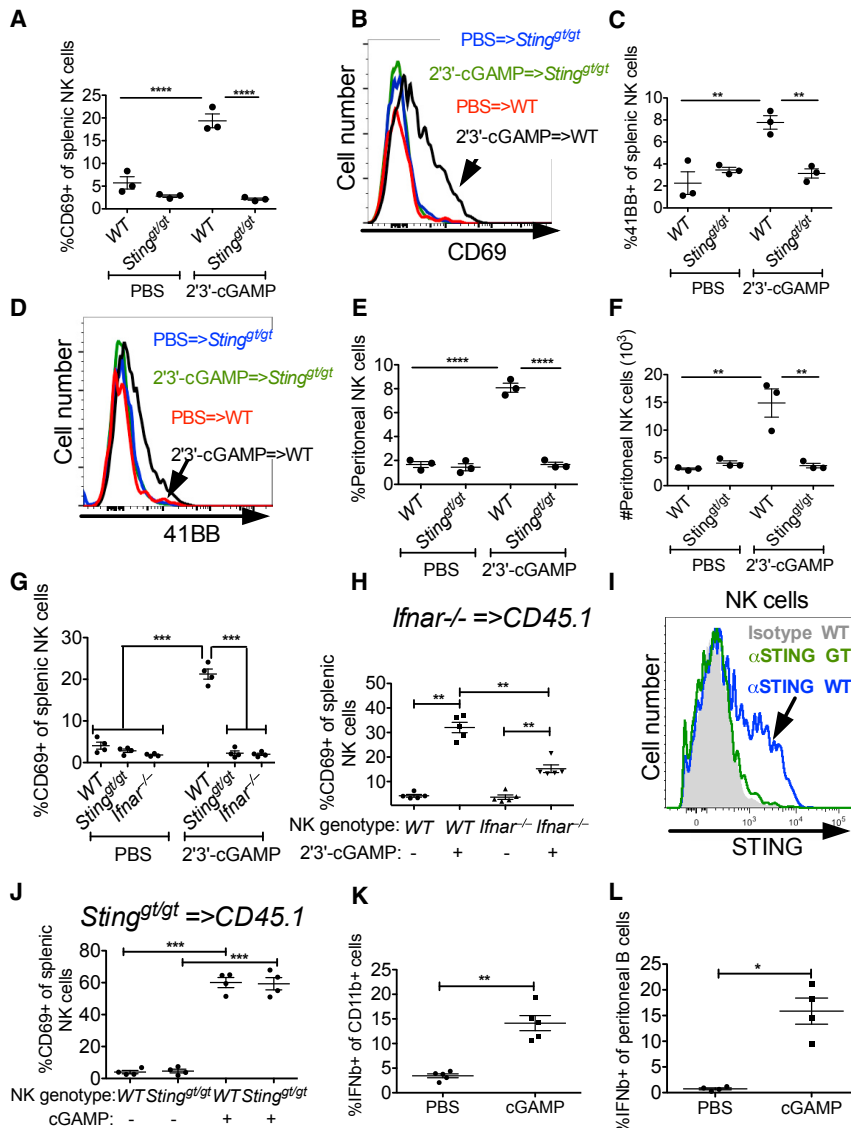


Figure 5. Exogenous 2'3'-cGAMP Activates NK Cells in a Cell-Extrinsic Fashion

(A–G) 200 nmol 2'3'-cGAMP was injected intraperitoneally into WT, *Sting*^{gt/gt}, or *Ifnar*^{-/-} mice (n = 3 or 4), and 18 hr later splenocytes were analyzed by flow cytometry. Percentages of CD69⁺ (A and G) and 4-1BB⁺ (C) splenic NK cells and representative CD69 (B) and 4-1BB (D) staining profiles are shown. Analysis of peritoneal wash cells collected from 2'3'-cGAMP-injected mice shows the percentages (E) and absolute numbers (F) of peritoneal NK cells.

(H and J) 30 × 10⁶ *Ifnar*^{-/-} (H) or *Sting*^{gt/gt} (J) splenocytes were transferred intravenously into CD45.1 mice, and the mice were challenged intraperitoneally with 200 nmol 2'3'-cGAMP. 12 hr later, splenocytes were harvested and donor and host NK cells were analyzed for CD69 expression. (I) Gated NK cells from WT and *Sting*^{gt/gt} mice were stained intracellularly for STING expression.

(K and L) 500 μg (696 nmol) 2'3'-cGAMP was injected into 7-day established RMA-S tumors (K) or intraperitoneally in non-tumor-bearing mice (L), and 1 hr later, the tumors (K) or peritoneal wash cells (L) were harvested for analysis. Cells were incubated with brefeldin and monensin for 5 hr before intracellular IFN-β staining. Shown are the results for CD11b⁺ tumor myeloid cells (negative for CD3, CD19, NKp46, and Ly6G) (K) and peritoneal B cells (L).

Results are representative of two to four independent experiments. For cGAMP injections, data were analyzed by one-way ANOVA with Bonferroni's correction for multiple comparisons. Error bars represent means ± SEM.

rejected in a STING-dependent fashion *in vivo*, whereas WT tumor cells were partially rejected as before (Figures 6E and 6F). Restoration with WT cGAS restored the STING-dependent tumor rejection response, whereas restoration with catalytically inactive cGAS did not (Figures 6G–6H and Figures S3J and S3K), confirming that the defect was due to differences in cGAS enzymatic activity and not to other clonally variable properties of the tumor cells. Together, these data indicate that the NK-mediated rejection of B16-BL6 tumors requires active cGAS in tumor cells and STING expression in host cells.

CGAS Expression Correlates with Immune Activation and Improved Survival in Melanoma

We sought to evaluate the clinical relevance of our findings by analyzing cGAS expression in tumors with publicly available data from The Cancer Genome Atlas (TCGA). Because our find-

ings suggest a role for CGAS expression in tumors in inducing anti-tumor responses, we focused on melanoma, which tends to be a relatively immunogenic tumor type.

We proceeded to look for gene expression relationships consistent with the induction of immune activation by cGAS expression. As a control comparison, we examined pairs of genes that are known to be co-expressed, such as *CD3E* and *CD3D*, which did indeed display a significant although imperfect correlation (Figure 7A). Given that CGAS-induced genes are also induced by other upstream sensors, we opted to use cGAS expression as a surrogate marker for cGAS activation on the basis of the reasoning that higher cGAS expression leads to a stronger activation of the pathway. Immune activation was quantified on the basis of the expression of several genes, including *CD69*, *IFNG*, *TNF*, *GZMA*, *GZMB*, and *IFIT1*. We found strong correlations between cGAS expression levels and expression of immune-activation genes (Figure 7B and Figure S4). We could not assess NK cell activation directly because there are no immune activation markers that are specific to NK cells. We could, however, quantify NK cell infiltration by examining expression of several genes that are preferentially expressed by NK cells including: *KIR2DL4*, *NCR1*, *KLRD1*, *KLRC1*, *KLRC2*, *KLRC3*, *KLRC4*, *KLRB1*, and

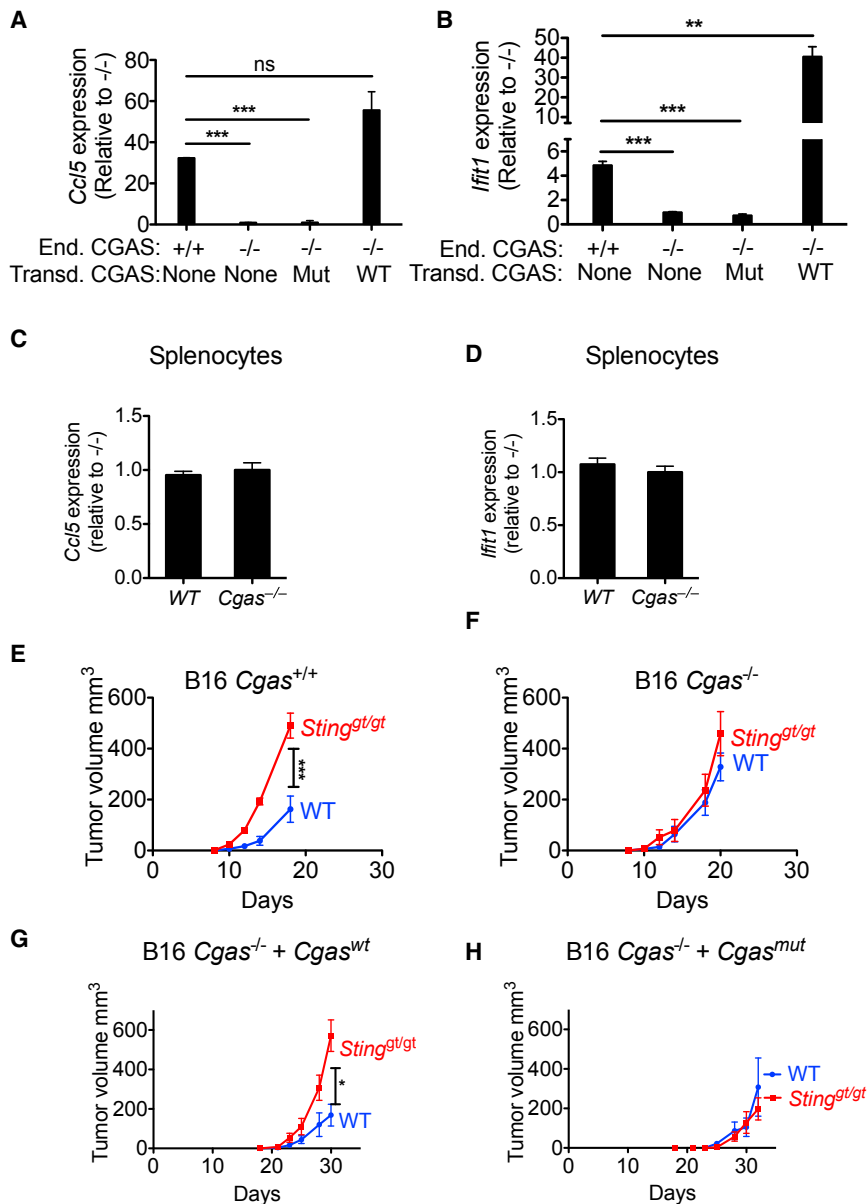


Figure 6. Constitutive cGAS Activation in Tumor Cells Leads to Tumor Rejection Dependent on Host STING

(A and B) qRT-PCR analysis of *Ccl5* (A) and *Ifit1* (B) expression levels in B16-BL6-*Cgas*^{+/+}, B16-*Cgas*^{-/-}, or B16-*Cgas*^{-/-} tumor cells transduced with either active (*Cgas*^{WT}) or inactive (*Cgas*^{mut}) *Cgas* expression vector.

(C and D) qRT-PCR analysis of *Ccl5* (C) and *Ifit1* (D) expression levels in splenocytes isolated from WT or *Cgas*^{-/-} mice. Results are representative of three to six independent experiments, and data consist of three technical replicates. Fold expression is shown in relation to that of mutant cells. Statistical significance was assessed by two-tailed t tests.

(E–H) Tumor cells (10^5) were injected subcutaneously into WT or *Sting*^{gt/gt} mice, and tumor growth was monitored as in Figure 1. Each group contained four to six mice, and results are representative of two independent experiments. Injected tumor cells were B16-BL6-*CGAS*^{+/+} cells (E), B16-BL6-*Cgas*^{-/-} cells (F), or B16-BL6-*Cgas*^{-/-} cells transduced with an active (*Cgas*^{WT}, G) or inactive (*Cgas*^{mut}, H) cGAS expression vector. Statistical significance was assessed as in Figure 1.

Error bars represent means \pm SEM.

DISCUSSION

Two major conclusions can be derived from our findings. First, NK-dependent rejection of tumor cells is largely reliant on the activation of STING in non-tumor cells, at least in some cases. Second, steady-state activation of cGAS in tumor cells rather than cGAS activation in host cells is required for NK cell responses against tumors, suggesting that tumor-derived cGAMP is responsible for STING activation and could be transferred to non-cancerous cells to activate the response. Thus, aberrant cGAS activation in tumors boosts anti-tumor immune

responses. Notably, rejection of normal MHC-I-deficient bone marrow cells by NK cells did not require host STING expression, nor did T-cell-mediated skin allograft rejection (Woo et al., 2014). These findings support the conclusion that the immunogenicity of tumor cells in both the NK and T cell responses could be amplified by the cGAS-STING pathway, although it remains possible that other differences between these tumor cells and normal cells or in the experimental protocols could account for the different outcomes.

KLRK1. There was a significant correlation between cGAS and expression levels of the various NK cell receptors (Figures 7C–7D and Figure S5). We then asked whether increased cGAS expression is associated with expression of ligands that render cells NK sensitive. There was a significant correlation between cGAS expression and expression of the NKG2D ligands ULBP1 and ULBP3 (Figures 7E and 7F), in accordance with an earlier report that showed that cGAS-STING activation can lead to expression of NKG2D ligands (Lam et al., 2014). Finally, in melanoma patients, we demonstrated a significant correlation between cGAS expression levels and survival and between NK cell receptor (including *NCR1*) expression levels and survival (Figures 7G–7H and Figure S6). These data are consistent with a role for cGAS in the induction of anti-tumor responses in melanoma patients in accordance with our model.

The evidence that the cGAS-STING pathway underlies NK cell responses to tumors provides a new foundation for the decades-old field of natural cytotoxicity to tumors (Herberman et al., 1975; Kiessling et al., 1975). The findings provide a mechanism for amplifying NK cell responses to aberrant tumor cells, analogous to the role of pattern-recognition receptors, including cGAS, in amplifying other immune responses to pathogens. In viral

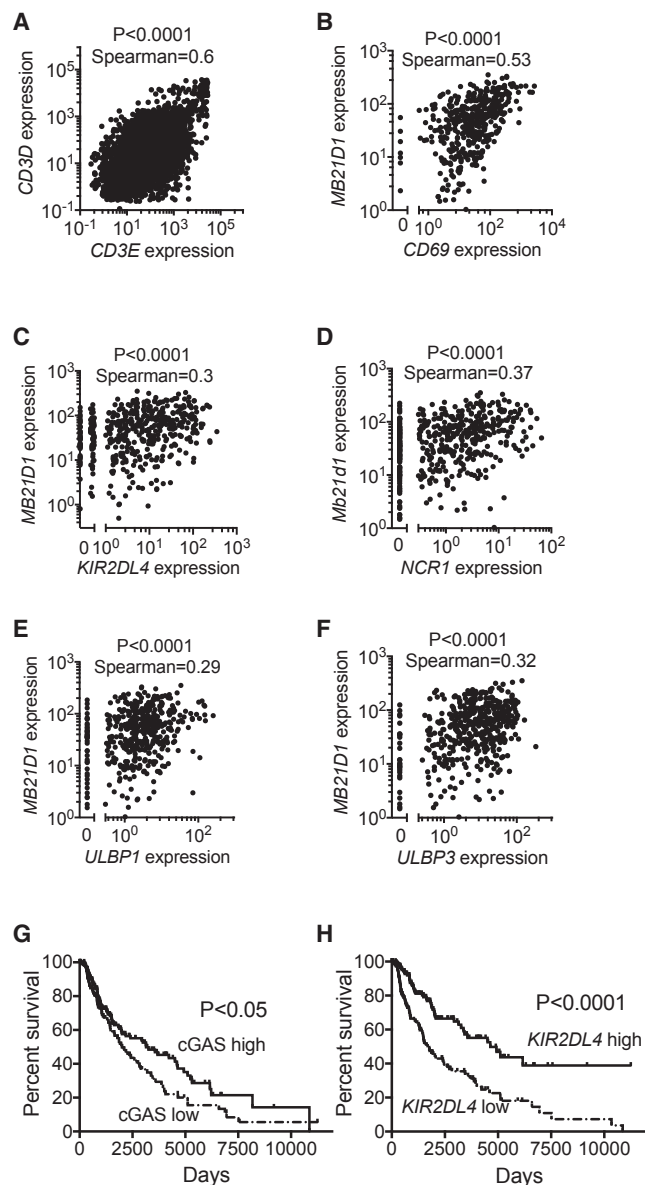


Figure 7. Clinical Correlations with cGAS and NK Cells in Human Melanoma

(A–F) Plots of (A) CD3E versus CD3D expression across all cancers, (B) cGAS versus CD69 expression in melanoma, (C) cGAS versus KIR2DL4 expression in melanoma, (D) cGAS versus NCR1 expression in melanoma, (E) cGAS versus ULBP1 expression in melanoma, and (F) cGAS versus ULBP3 expression in melanoma.

(G) Kaplan-Meier plot of melanoma patient survival; patients are segmented by cGAS expression (highest and lowest thirds).

(H) Kaplan-Meier plot of melanoma patient survival; patients are segmented by KIR2DL4 expression (highest and lowest thirds).

All data were obtained from The Cancer Genome Atlas (TCGA). For correlations of expression, statistical significance was assessed with the Spearman coefficient. For survival analysis, statistical significance was assessed with the log-rank test.

infections, cGAS, RNA sensors, and Toll-like receptors play an important role in promoting anti-viral responses, but the role of such receptors in triggering spontaneous NK responses to

tumors has not been previously demonstrated. STING, which is downstream of cGAS, is important in CD8⁺ T cell responses to tumors (Woo et al., 2014), and it will be interesting to address whether tumor or host cGAS is similarly necessary for such T cell responses.

It has previously been proposed that tumor cells activate the cGAS-STING pathway *in vivo* through the transfer of tumor cell DNA into host cells (Klarquist et al., 2014; Ohkuri et al., 2014; Woo et al., 2014), although the mechanism whereby tumor DNA might access the cytosol and the causal relationship between DNA transfer and STING activation have not been established. The DNA transfer model predicts that cGAS, like STING, is required in host cells, contrary to our results. Instead, our results suggest that cGAMP is produced in tumor cells and could be transferred to host cells to trigger STING, resulting in the production of cytokines (such as type I IFN), which are known to enhance NK cell cytotoxicity. cGAMP transfer can occur in the context of viral infection, at least in an *in vitro* setting, through a variety of mechanisms, including transfer through gap junctions, transfer through viral particles, and transfer via membrane fusion (Ablasser et al., 2013b; Gentili et al., 2015; Xu et al., 2016). *In vivo*, cGAMP transfer through gap junctions between tumor cells and astrocytes promotes brain metastases, although the underlying mechanisms are not clear (Chen et al., 2016a), but evidence supporting a role for cGAMP transfer *in vivo* in inducing immune responses is lacking.

Our data suggest that cGAMP is transferred from tumor cells to host cells to initiate the response. Injected 2′3′-cGAMP induced IFN-β expression in CD11b⁺ cells within tumors, but not in neutrophils, NK cells, or T cells, suggesting that CD11b⁺ cells are candidates for receiving 2′3′-cGAMP during anti-tumor responses. However, it remains possible that other cell types participate; for example, B cells have not been previously suggested to act as 2′3′-cGAMP sensors but are capable of responding to it. More generally, it is plausible that different cell types play roles in different tumor microenvironments. Although we have demonstrated that extracellular cGAMP can trigger host STING and initiate an NK cell response, additional studies will be necessary to establish whether and how cGAMP is transferred from tumor cells to host cells.

STING can be activated in response to DNA damage, which could explain why cGAMP is produced in tumor cells. DNA damage and activation of the DNA damage response are a hallmark of cancer (Gasser and Raulet, 2006b; Hanahan and Weinberg, 2000), and some tumor cell lines, such as YAC-1, EμM1, TRAMPC2, DU145, and PC-3, contain detectable cytosolic DNA (Ho et al., 2016; Lam et al., 2014; Shen et al., 2015) and spontaneously produce cytokines in culture in a STING-dependent manner. Together with our finding that the cGAS-STING pathway is constitutively active in B16 and THP1 cells, these data suggest that constitutive activation of the cGAS-STING pathway is fairly common and most likely occurs in many tumors. We propose that genomic abnormalities and the consequent activation of the DNA sensing pathway help to mark these cells as abnormal and trigger cGAS in tumor cells. This leads to STING activation in host cells and eventually mobilizes a sufficiently potent NK cell response to reject the tumors (completely or partially depending on the system). This proposal would establish cGAS activation as a distinguishing characteristic of tumor cells and would explain why rejection of non-transformed MHC-I-deficient bone marrow

cells does not require host STING. It is plausible that rejection of non-transformed cell grafts requires only weak NK cell activity that is independent of host STING activation, whereas rejection of growing tumor cells requires a more potent or sustained response that depends on factors downstream of host STING.

Our model positions cGAS expression in tumors as a major determinant of tumor immunogenicity. Interestingly, cGAS is inactivated in certain tumors (Xia et al., 2016a; Xia et al., 2016b). Loss of cGAS from tumor cells might be a mechanism by which tumors evolve to escape the cGAS-STING-dependent immune response we describe here. It is difficult to envisage, however, how loss of cGAMP production in one cell would provide a fitness advantage to that cell if tumor cells nearby continued to produce cGAMP. Alternatively, loss of cGAS expression by tumor cells could provide cell-intrinsic benefits to tumor cells, e.g., permit the tumor cell to circumvent senescence (Glück et al., 2017; Yang et al., 2017) or prevent immunostimulatory NKG2D ligand expression (Lam et al., 2014). Regardless, our results imply that heterogeneity in cGAS activity across tumors could be an important predictor of cancer prognosis and response to treatment. Indeed, our results reinforce the rationale for the use of exogenous cyclic-dinucleotides for tumor immunotherapy (Corrales et al., 2015) and suggest that NK cells could play an important role in mediating the anti-tumor effects of the treatment.

STAR★METHODS

Detailed methods are provided in the online version of this paper and include the following:

- KEY RESOURCES TABLE
- CONTACT FOR REAGENT AND RESOURCE SHARING
- EXPERIMENTAL MODEL AND SUBJECT DETAILS
 - Mouse Strains
 - Cell Lines and Culture Conditions
- METHOD DETAILS
 - *In Vivo* Tumor Models
 - *In Vivo* Stimulation with cGAMP
 - *In Vivo* Rejection Assay
 - HSV1 Infections
 - *Cgas* Mutant Mice
 - *Cgas*^{-/-} Tumor Cells
 - Plasmids, Mutagenesis, and Transduction
 - Flow Cytometry
 - DNA Transfections and DNA Damage Induction
 - NK Cell Responsiveness Assay
 - Quantitative RT-PCR
 - Type I IFN Bioassay
- QUANTIFICATION AND STATISTICAL ANALYSIS
 - Clinical Data Analysis

SUPPLEMENTAL INFORMATION

Supplemental Information includes six figures, one table and can be found with this article online at <https://doi.org/10.1016/j.immuni.2018.09.016>.

ACKNOWLEDGMENTS

We thank L. Zhang and T. Trevino for their assistance in the lab and members of the Raulet and Vance labs for discussions. Hector Nolla and Alma Valeros

provided assistance with cell sorting. We acknowledge the technical support of Chulho Kang and the Cancer Research Laboratory Gene Targeting Facility with the generation of *Cgas*-deficient mice. This research was supported by NIH grant R01-AI0113041 to D.H.R. R.E.V. is supported by an investigator award from the Howard Hughes Medical Institute and by NIH grants AI075039 and AI063302.

AUTHOR CONTRIBUTIONS

A.M., A.J.M., M.L.V., and L.W. conducted the experiments, and A.M., R.E.V., and D.H.R. designed the experiments and wrote the paper.

DECLARATION OF INTERESTS

D.H.R. is a co-founder of Dragonfly Therapeutics and served or serves on the scientific advisory boards of Dragonfly, Aduro Biotech, Innate Pharma, and Ignite Immunotherapy; he has a financial interest in all four companies and could benefit from commercialization of the results of this research. R.E.V. is an inventor on US patent US 9,724,408, "Compositions and Methods for Activating Stimulator of Interferon Gene-Dependent Signaling."

Received: February 10, 2018

Revised: June 18, 2018

Accepted: September 21, 2018

Published: October 16, 2018

REFERENCES

- Ablasser, A., Goldeck, M., Cavlari, T., Deimling, T., Witte, G., Röhl, I., Hopfner, K.P., Ludwig, J., and Hornung, V. (2013a). cGAS produces a 2'-5'-linked cyclic dinucleotide second messenger that activates STING. *Nature* 498, 380–384.
- Ablasser, A., Schmid-Burgk, J.L., Hemmerling, I., Horvath, G.L., Schmidt, T., Latz, E., and Hornung, V. (2013b). Cell intrinsic immunity spreads to bystander cells via the intercellular transfer of cGAMP. *Nature* 503, 530–534.
- Brzostek-Racine, S., Gordon, C., Van Scoy, S., and Reich, N.C. (2011). The DNA damage response induces IFN. *J. Immunol.* 187, 5336–5345.
- Cerami, E., Gao, J., Dogrusoz, U., Gross, B.E., Sumer, S.O., Aksoy, B.A., Jacobsen, A., Byrne, C.J., Heuer, M.L., Larsson, E., et al. (2012). The cBio cancer genomics portal: An open platform for exploring multidimensional cancer genomics data. *Cancer Discov.* 2, 401–404.
- Chaix, J., Tessmer, M.S., Hoebe, K., Fuséri, N., Ryffel, B., Dalod, M., Alexopoulou, L., Beutler, B., Brossay, L., Vivier, E., and Walzer, T. (2008). Cutting edge: Priming of NK cells by IL-18. *J. Immunol.* 181, 1627–1631.
- Chen, Q., Boire, A., Jin, X., Valiente, M., Er, E.E., Lopez-Soto, A., Jacob, L., Patwa, R., Shah, H., Xu, K., et al. (2016a). Carcinoma-astrocyte gap junctions promote brain metastasis by cGAMP transfer. *Nature* 533, 493–498.
- Chen, Q., Sun, L., and Chen, Z.J. (2016b). Regulation and function of the cGAS-STING pathway of cytosolic DNA sensing. *Nat. Immunol.* 17, 1142–1149.
- Corrales, L., Glickman, L.H., McWhirter, S.M., Kanne, D.B., Sivick, K.E., Katibah, G.E., Woo, S.R., Lemmens, E., Banda, T., Leong, J.J., et al. (2015). Direct activation of STING in the tumor microenvironment leads to potent and systemic tumor regression and immunity. *Cell Rep.* 11, 1018–1030.
- Deng, W., Gowen, B.G., Zhang, L., Wang, L., Lau, S., Iannello, A., Xu, J., Rovis, T.L., Xiong, N., and Raulet, D.H. (2015). Antitumor immunity. A shed NKG2D ligand that promotes natural killer cell activation and tumor rejection. *Science* 348, 136–139.
- Diefenbach, A., Jensen, E.R., Jamieson, A.M., and Raulet, D.H. (2001). Rae1 and H60 ligands of the NKG2D receptor stimulate tumour immunity. *Nature* 413, 165–171.
- Diner, E.J., Burdette, D.L., Wilson, S.C., Monroe, K.M., Kellenberger, C.A., Hyodo, M., Hayakawa, Y., Hammond, M.C., and Vance, R.E. (2013). The innate immune DNA sensor cGAS produces a noncanonical cyclic dinucleotide that activates human STING. *Cell Rep.* 3, 1355–1361.
- Gao, D., Wu, J., Wu, Y.T., Du, F., Aroh, C., Yan, N., Sun, L., and Chen, Z.J. (2013a). Cyclic GMP-AMP synthase is an innate immune sensor of HIV and other retroviruses. *Science* 341, 903–906.

- Gao, P., Ascano, M., Wu, Y., Barchet, W., Gaffney, B.L., Zillinger, T., Serganov, A.A., Liu, Y., Jones, R.A., Hartmann, G., et al. (2013b). Cyclic [G(2',5')pA(3',5')p] is the metazoan second messenger produced by DNA-activated cyclic GMP-AMP synthase. *Cell* 153, 1094–1107.
- Gao, P., Ascano, M., Zillinger, T., Wang, W., Dai, P., Serganov, A.A., Gaffney, B.L., Shuman, S., Jones, R.A., Deng, L., et al. (2013c). Structure-function analysis of STING activation by c[G(2',5')pA(3',5')p] and targeting by antiviral DMXAA. *Cell* 154, 748–762.
- Gasser, S., and Raulet, D. (2006a). The DNA damage response, immunity and cancer. *Semin. Cancer Biol.* 16, 344–347.
- Gasser, S., and Raulet, D.H. (2006b). The DNA damage response arouses the immune system. *Cancer Res.* 66, 3959–3962.
- Gentili, M., Kowal, J., Tkach, M., Satoh, T., Lahaye, X., Conrad, C., Boyron, M., Lombard, B., Durand, S., Kroemer, G., et al. (2015). Transmission of innate immune signaling by packaging of cGAMP in viral particles. *Science* 349, 1232–1236.
- Glas, R., Franksson, L., Une, C., Eloranta, M.L., Ohlén, C., Orn, A., and Kärre, K. (2000). Recruitment and activation of natural killer (NK) cells in vivo determined by the target cell phenotype. An adaptive component of NK cell-mediated responses. *J. Exp. Med.* 191, 129–138.
- Glück, S., Guey, B., Gulen, M.F., Wolter, K., Kang, T.W., Schmacke, N.A., Bridgeman, A., Rehwinkel, J., Zender, L., and Ablasser, A. (2017). Innate immune sensing of cytosolic chromatin fragments through cGAS promotes senescence. *Nat. Cell Biol.* 19, 1061–1070.
- Guia, S., Cognet, C., de Beaucoudrey, L., Tessmer, M.S., Jouanguy, E., Berger, C., Filipe-Santos, O., Feinberg, J., Camcioglu, Y., Levy, J., et al. (2008). A role for interleukin-12/23 in the maturation of human natural killer and CD56+ T cells in vivo. *Blood* 111, 5008–5016.
- Hanahan, D., and Weinberg, R.A. (2000). The hallmarks of cancer. *Cell* 100, 57–70.
- Härtlova, A., Ertmann, S.F., Raffi, F.A., Schmalz, A.M., Resch, U., Anugula, S., Lienenklaus, S., Nilsson, L.M., Kröger, A., Nilsson, J.A., et al. (2015). DNA damage primes the type I interferon system via the cytosolic DNA sensor STING to promote anti-microbial innate immunity. *Immunity* 42, 332–343.
- Herberman, R.B., Nunn, M.E., and Lavrin, D.H. (1975). Natural cytotoxic reactivity of mouse lymphoid cells against syngeneic acid allogeneic tumors. I. Distribution of reactivity and specificity. *Int. J. Cancer* 16, 216–229.
- Ho, S.S., Zhang, W.Y., Tan, N.Y., Khatoo, M., Suter, M.A., Tripathi, S., Cheung, F.S., Lim, W.K., Tan, P.H., Ngeow, J., and Gasser, S. (2016). The DNA structure-specific endonuclease MUS81 mediates DNA sensor STING-dependent host rejection of prostate cancer cells. *Immunity* 44, 1177–1189.
- Ishii, K.J., Coban, C., Kato, H., Takahashi, K., Torii, Y., Takeshita, F., Ludwig, H., Sutter, G., Suzuki, K., Hemmi, H., et al. (2006). A Toll-like receptor-independent antiviral response induced by double-stranded B-form DNA. *Nat. Immunol.* 7, 40–48.
- Ishikawa, H., Ma, Z., and Barber, G.N. (2009). STING regulates intracellular DNA-mediated, type I interferon-dependent innate immunity. *Nature* 461, 788–792.
- Kärre, K. (2008). Natural killer cell recognition of missing self. *Nat. Immunol.* 9, 477–480.
- Kiessling, R., Klein, E., and Wigzell, H. (1975). “Natural” killer cells in the mouse. I. Cytotoxic cells with specificity for mouse Moloney leukemia cells. Specificity and distribution according to genotype. *Eur. J. Immunol.* 5, 112–117.
- Klarquist, J., Hennies, C.M., Lehn, M.A., Reboulet, R.A., Feau, S., and Janssen, E.M. (2014). STING-mediated DNA sensing promotes antitumor and autoimmune responses to dying cells. *J. Immunol.* 193, 6124–6134.
- Lam, A.R., Bert, N.L., Ho, S.S., Shen, Y.J., Tang, L.F., Xiong, G.M., Croxford, J.L., Koo, C.X., Ishii, K.J., Akira, S., et al. (2014). RAE1 ligands for the NKG2D receptor are regulated by STING-dependent DNA sensor pathways in lymphoma. *Cancer Res.* 74, 2193–2203.
- Lanier, L.L. (2005). NK cell recognition. *Annu. Rev. Immunol.* 23, 225–274.
- Marcus, A., Gowen, B.G., Thompson, T.W., Iannello, A., Ardolino, M., Deng, W., Wang, L., Shifrin, N., and Raulet, D.H. (2014). Recognition of tumors by the innate immune system and natural killer cells. *Adv. Immunol.* 122, 91–128.
- Mortier, E., Advincula, R., Kim, L., Chmura, S., Barrera, J., Reizis, B., Malynn, B.A., and Ma, A. (2009). Macrophage- and dendritic-cell-derived interleukin-15 receptor alpha supports homeostasis of distinct CD8+ T cell subsets. *Immunity* 31, 811–822.
- Narni-Mancinelli, E., Chaix, J., Fenis, A., Kerdiles, Y.M., Yessaad, N., Reynders, A., Gregoire, C., Luche, H., Ugolini, S., Tomasello, E., et al. (2011). Fate mapping analysis of lymphoid cells expressing the Nkp46 cell surface receptor. *Proc. Natl. Acad. Sci. USA* 108, 18324–18329.
- Ohkuri, T., Ghosh, A., Kosaka, A., Zhu, J., Ikeura, M., David, M., Watkins, S.C., Sarkar, S.N., and Okada, H. (2014). STING contributes to anti glioma immunity via triggering type I IFN signals in the tumor microenvironment. *Cancer Immunol. Res.* 2, 1199–1208.
- Raulet, D.H. (2004). Interplay of natural killer cells and their receptors with the adaptive immune response. *Nat. Immunol.* 5, 996–1002.
- Raulet, D.H., Gasser, S., Gowen, B.G., Deng, W., and Jung, H. (2013). Regulation of ligands for the NKG2D activating receptor. *Annu. Rev. Immunol.* 31, 413–441.
- Sauer, J.D., Sotelo-Troha, K., von Moltke, J., Monroe, K.M., Rae, C.S., Brubaker, S.W., Hyodo, M., Hayakawa, Y., Woodward, J.J., Portnoy, D.A., and Vance, R.E. (2011). The N-ethyl-N-nitrosourea-induced Goldenticket mouse mutant reveals an essential function of Sting in the in vivo interferon response to *Listeria monocytogenes* and cyclic dinucleotides. *Infect. Immun.* 79, 688–694.
- Shen, Y.J., Le Bert, N., Chitre, A.A., Koo, C.X., Nga, X.H., Ho, S.S., Khatoo, M., Tan, N.Y., Ishii, K.J., and Gasser, S. (2015). Genome-derived cytosolic DNA mediates type I interferon-dependent rejection of B cell lymphoma cells. *Cell Rep.* 11, 460–473.
- Stetson, D.B., and Medzhitov, R. (2006). Recognition of cytosolic DNA activates an IRF3-dependent innate immune response. *Immunity* 24, 93–103.
- Wang, H., Yang, H., Shivalila, C.S., Dawlaty, M.M., Cheng, A.W., Zhang, F., and Jaenisch, R. (2013). One-step generation of mice carrying mutations in multiple genes by CRISPR/Cas-mediated genome engineering. *Cell* 153, 910–918.
- Woo, S.R., Fuertes, M.B., Corrales, L., Spranger, S., Furdyna, M.J., Leung, M.Y., Duggan, R., Wang, Y., Barber, G.N., Fitzgerald, K.A., et al. (2014). STING-dependent cytosolic DNA sensing mediates innate immune recognition of immunogenic tumors. *Immunity* 41, 830–842.
- Wu, J., Sun, L., Chen, X., Du, F., Shi, H., Chen, C., and Chen, Z.J. (2013). Cyclic GMP-AMP is an endogenous second messenger in innate immune signaling by cytosolic DNA. *Science* 339, 826–830.
- Xia, T., Konno, H., Ahn, J., and Barber, G.N. (2016a). Deregulation of STING signaling in colorectal carcinoma constrains DNA damage responses and correlates with tumorigenesis. *Cell Rep.* 14, 282–297.
- Xia, T., Konno, H., and Barber, G.N. (2016b). Recurrent loss of STING signaling in melanoma correlates with susceptibility to viral oncolysis. *Cancer Res.* 76, 6747–6759.
- Xu, S., Ducroux, A., Ponnuram, A., Vieyres, G., Franz, S., Müsken, M., Zillinger, T., Malassa, A., Ewald, E., Hornung, V., et al. (2016). cGAS-mediated innate immunity spreads intercellularly through HIV-1 Env-induced membrane fusion sites. *Cell Host Microbe* 20, 443–457.
- Yang, H., Wang, H., Ren, J., Chen, Q., and Chen, Z.J. (2017). cGAS is essential for cellular senescence. *Proc. Natl. Acad. Sci. USA* 114, E4612–E4620.
- Yokoyama, W.M., and Plougastel, B.F. (2003). Immune functions encoded by the natural killer gene complex. *Nat. Rev. Immunol.* 3, 304–316.
- Zhang, X., Shi, H., Wu, J., Zhang, X., Sun, L., Chen, C., and Chen, Z.J. (2013). Cyclic GMP-AMP containing mixed phosphodiester linkages is an endogenous high-affinity ligand for STING. *Mol. Cell* 51, 226–235.
- Zhu, Q., Man, S.M., Gurung, P., Liu, Z., Vogel, P., Lamkanfi, M., and Kanneganti, T.D. (2014). Cutting edge: STING mediates protection against colorectal tumorigenesis by governing the magnitude of intestinal inflammation. *J. Immunol.* 193, 4779–4782.

STAR★METHODS

KEY RESOURCES TABLE

REAGENT or RESOURCE	SOURCE	IDENTIFIER
Antibodies		
NK1.1 (PK136) – BV711	BioLegend	108745; RRID: AB_2563286
CD3 ϵ (145-2C11) – PE/Cy5	BioLegend	100309; RRID: AB_312674
CD19 (6D5) – BV605	BioLegend	115540; RRID: AB_2563067
CD45.1 (A20) – Percp/Cy5.5	BioLegend	110728; RRID: AB_893346
CD45.2 (104) – BUV395	BD	564616
IFN- γ (XMG1.2) – PE	BioLegend	505808; RRID: AB_315402
CD107a (1D4B) – A647	BioLegend	121609; RRID: AB_571990
NKG2D (CX5) – PE	BioLegend	130207; RRID: AB_1227713
NKp46 (29A1.4) – FITC	BioLegend	137606; RRID: AB_2298210
CD11b (M1/70) – PE/Cy7	BioLegend	101216; RRID: AB_312799
CD69 (H1.2F3) – PE/Dazzle594	BioLegend	104536; RRID: AB_2565583
4-1BB (17B5) – PE	BioLegend	106106; RRID: AB_2287565
STING (clone 41)	Millipore	MABF213
Bacterial and Virus Strains		
HSV1	ATCC	ATCC VR-1487 (KOS)
Chemicals, Peptides, and Recombinant Proteins		
2'3'-cGAMP	Produced in house	N/A
Vaccinia 70-mer	InvivoGen	tlrl-vav70n
ISD DNA	InvivoGen	tlrl-isdn
Herring Testes HT-DNA	Sigma-Aldrich	D6898
Poybrene	Sigma-Aldrich	TR-1003
Cytofix/Cytoperm	BD	554722
GolgiPlug	BD	555029
GolgiStop	BD	554724
CFSE	Thermo Fisher Scientific	C34554
Cytarabine ARA-C	Cayman Chemical	16069
Critical Commercial Assays		
QuikChange Site Mutagenesis kit	Agilent technologies	210514
RNAeasy Mini kit	QIAGEN	74104
iScript reverse transcriptase	Bio-Rad	1708841
SSO-Fast Eva Green Supermix	Bio-Rad	1725203
Experimental Models: Cell Lines		
293T	ATCC	CRL-3216
B16-BL6	Laboratory of James P. Allison	N/A
B16-BL6- <i>Cgas</i> ^{-/-}	This paper	N/A
RMA-S	Laboratory of Klas Karre	N/A
RMA	Laboratory of Klas Karre	N/A
RMA-RAE-1 ϵ	Produced in house	N/A
THP1	InvivoGen	thpd-nfis
THP1- <i>TMEM173</i> ^{-/-}	InvivoGen	thpd-kostg
MC38-GFP/Luc	Laboratory of Dr. Michel Dupage	N/A
Experimental Models: Organisms/Strains		
C57BL/6J	Jackson Laboratory	000664
C57BL/6J <i>Tmem173</i> ^{-/-}	Jackson Laboratory	017537

(Continued on next page)

Continued

REAGENT or RESOURCE	SOURCE	IDENTIFIER
C57BL/6J <i>Cgas</i> ^{-/-}	This paper	N/A
C57BL/6J <i>Ifnar1</i> ^{-/-}	Jackson Laboratory	028228
C57BL/6J <i>Irf3</i> ^{-/-}	Laboratory of Dr. T. Taniguchi	N/A
C57BL/6J Ly5.1	Jackson Laboratory	002014
C57BL/6J <i>B2m</i> ^{-/-}	Jackson Laboratory	002087
C57BL/6J <i>Rag2</i> ^{-/-}	Jackson Laboratory	008449
C57BL/6J <i>Nkp46</i> ^{iCRE}	Laboratory of Dr. Eric Vivier	N/A
C57BL/6J R26-LSL-DTA	Jackson Laboratory	009669
Oligonucleotides		
For synthetic DNA sequences, see Table S1	N/A	N/A
Recombinant DNA		
Cas9 mRNA	TriLink	L-7606
MSCV2.2	Addgene	60206
Software and Algorithms		
Prism	GraphPad Prism software	Version 7.0
FlowJo	Tree Star software	Version 10

CONTACT FOR REAGENT AND RESOURCE SHARING

Further information and requests for resources and reagents should be delivered to and will be fulfilled by the Lead Contact, David H. Raulet (raulet@berkeley.edu). Completed Material Transfer Agreements may be required for obtaining mutant mice or cell lines generated in this study.

EXPERIMENTAL MODEL AND SUBJECT DETAILS**Mouse Strains**

All experiments were carried out with mice on the C57BL/6J background. C57BL/6J breeder mice were obtained from Jackson Laboratories. Goldenticket *Sting*^{gt/gt} mutant mice were previously described ([Sauer et al., 2011](#)). *Rag2*^{-/-} mice were crossed to *Sting*^{gt/gt} mice to generate *Rag2*^{-/-}*Sting*^{gt/gt} mice. *Irf3*^{-/-} mice were kindly provided by T. Taniguchi (University of Tokyo, Tokyo, Japan). *B2m*^{-/-}, and *B2m*-Ly5.1 mice were bred in our facility. Sex and age-matched (6 to 14 weeks old) mice were used in experiments. *Nkp46*^{iCre} mice, which express improved CRE recombinase in NK cells ([Narni-Mancinelli et al., 2011](#)), were generously provided by Eric Vivier. *Nkp46*^{iCre} mice were crossed to Rosa26-LSL-DTA (Jackson Laboratories) to generate NK-DTA mice, such that diphtheria toxin is expressed in nascent NK cells, resulting in NK cell-deficiency. *Cgas*^{-/-} mice were generated in house using CRISPR/Cas9 technology (see below for details). All experiments were approved by the UC Berkeley Animal Care and Use Committee.

Cell Lines and Culture Conditions

RMA-S, B16-BL6, RMA, RMA-RAE-1ε, MC38, THP1, and L929-ISRE cells were cultured in 5% CO₂ in RPMI containing 5% FBS (Omega Scientific), 0.2 mg/mL glutamine (Sigma-Aldrich), 100 u/mL penicillin (Thermo Fisher Scientific), 100 μg/mL streptomycin (Thermo Fisher Scientific), 10 μg/mL gentamicin sulfate (Lonza), 50 μM β-mercaptoethanol (EMD Biosciences), and 20 mM HEPES (Thermo Fisher Scientific). B16-BL6-*Cgas*^{-/-} cells were generated using CRISPR/Cas9 technology (see below for details). THP1 and THP1 *TMEM173*^{-/-} cells were obtained from Invivogen. MC38-GFP/Luc cells were kindly provided by Dr. Michel Dupage (UC Berkeley). All cell lines tested negative for mycoplasma contamination.

METHOD DETAILS**In Vivo Tumor Models**

Cells were resuspended in 100 μL of PBS, and injected subcutaneously. Tumor development and growth were monitored by caliper measurements. Tumor experiments typically included 4-6 mice per group. *In vivo* depletions of NK cells were done by intraperitoneal injections of 200 μg of PK136 antibody (recognizing NKR-P1C, also known as NK1.1) on day -1 prior to tumor injections, and once weekly thereafter. PK136 was purified and validated in our laboratory. NK cell-depletion was verified by flow cytometry.

In Vivo Stimulation with cGAMP

200 nmol of 2'3'-cGAMP (made in-house), as well as 2'3'-cGAMP provided by Aduro Biotech, was injected intraperitoneally. 12 or 18 hr later (depending on the experiment), splenocytes and peritoneal wash cells were harvested for analysis.

For intracellular cytokine staining studies, 500 μg (696 nmol) was injected either intratumorally or intraperitoneally. Tumor dissociates or peritoneal wash cells were isolated 1 hr later, and incubated for an additional 5 hr in the presence of brefeldin and monensin prior to intracellular cytokine staining.

In Vivo Rejection Assay

Bone marrow cells from CD45.1 *B2m*^{-/-} and CD45.1 WT mice were labeled with 10 μM CFSE or 1 μM CFSE, respectively. A mixture of 5×10^6 cells of each type was injected intravenously into recipient mice. Donor cell rejection was assessed 72 hr later by harvesting spleens and analyzing the percentages of CFSE^{high} and CFSE^{low} cells by flow cytometry.

HSV1 Infections

Age and sex-matched mice were infected intravenously with HSV-1 (ATCC), and monitored thereafter for paralysis and mortality. Moribund mice were euthanized in accordance with animal care guidelines.

Cgas Mutant Mice

Cgas mutant mice were generated using the CRISPR/Cas9 system. A gRNA was chosen to target the sequence 5'-TGACTCAGCGG ATTTCCCTCGTGG-3' in the second exon. A gRNA targeting the tyrosinase gene was also included, so that a coat color change would serve to indicate mice derived from embryos in which targeting was successful. The gRNAs were *in vitro* transcribed and injected together with Cas9 mRNA (Trilink) into single cell embryos as previously described (Wang et al., 2013). Several founder mice carrying frameshift mutations in the *Cgas* gene were identified, and a mouse carrying a 31 bp deletion was chosen. The mutation deleted the following sequence: 5'-CAAAGAATTCCACGAGGAAATCCGCTGAGT-3'. The mouse was backcrossed for eight generations to C57BL/6J mice in order to eliminate any tyrosinase mutations or other variants, before intercrossing to generate homozygous mutant mice. Whole genome SNP analysis (UC Davis, Mouse Biology Program) was used to confirm the mice were on a pure C57BL/6 background.

Cgas^{-/-} Tumor Cells

Cgas^{-/-} B16-BL6 cells were generated using the CRISPR/Cas9 system. Two gRNA flanking the first exon, including the first ATG codon, were selected. The gRNA were transfected together with Cas9 mRNA (Trilink) using lipofectamine2000 (Thermo Fisher Scientific). Cells were single cell-cloned, and mutant cells were identified using PCR. The genomic target sequences used for targeting were 5'-GTCAGATGTCGATTGATGCC-3' and 5'-GGTGACCTAAAGTAGTCGC-3'.

Plasmids, Mutagenesis, and Transduction

The retroviral *Cgas* expression plasmid, based on the MSCV2.2-IRES-EGFP backbone containing the complete open reading frame of mouse *Cgas* cDNA, was previously described (Diner et al., 2013). The plasmid was mutagenized to generate inactive *Cgas* (G198A/S199A) using QuikChange Site-directed mutagenesis kit according to the manufacturer's instructions. Retroviral supernatants were generated, and transductions were performed, as previously described (Deng et al., 2015). Briefly, 293T cells were co-transfected with plasmids encoding VSV gag/pol, Env, and pMSCV vectors using lipofectamine2000 (Thermo Fisher Scientific). Culture supernatants were collected 48 hr post-transfection, and added to pre-plated cells together with 8 $\mu\text{g}/\text{mL}$ polybrene. Transduced cells were selected based on GFP expression using an Influx cell sorter.

Flow Cytometry

Flow cytometry was performed using standard protocols. Briefly, cells were stained in 50 μL FACS buffer (2% BSA, 0.02% sodium azide, 1 mM EDTA). Dead cells were excluded using Live-Dead fixable stain kit using the manufacturer protocols. Cells were incubated for 20 min with 2.4G2 hybridoma supernatant (prepared in the lab) to block Fc γ RII/III receptors. For intracellular staining cells were fixed using Cytofix/Cytoperm (BD). Multicolor flow cytometry was performed on one of the following machines: LSR II, or LSR Fortessa or LSR X20 (BD). Data were analyzed using FlowJo software (Tree Star). NK cells were identified as CD3-, CD19-, NKp46+ cells.

DNA Transfections and DNA Damage Induction

All transfections were carried out with lipofectamine2000 (Thermo Fisher Scientific) according to the manufacturer's instructions. B16 cells were pre-plated at 5×10^5 /well in 6-well plates, and transfected with HT-DNA at a final concentration of 100 $\mu\text{g}/\text{mL}$, and cultured for 6 hr, before the cells were harvested for RNA isolation. Splenocytes were plated at 10^6 /well in 96-well plates, and transfected with Vaccina 70-mer at a final concentration of 0.5 $\mu\text{g}/\text{mL}$ for 4 hr. Afterward, the media was replaced with fresh media and the cells were incubated overnight. The following day media was harvested for the type I IFN bioassay. Splenocytes were also transfected with 2'3'-cGAMP in digitonin buffer for 30 min. Following transfection, the medium was replaced with fresh medium, and the cells were incubated for 7 hr before harvesting the culture supernatant for the type I IFN bioassay. DNA damage was induced by incubation with 50 μM ARA-C, and after 48 hr secreted type I IFN was measured using an IFN bioassay.

NK Cell Responsiveness Assay

High protein-binding flat bottom plates were pre-coated with 5 $\mu\text{g}/\text{mL}$ NKG2D (MI-6) or 5 $\mu\text{g}/\text{mL}$ NKp46 (29A1.4) antibody, or an isotype control antibody. Splenocytes were then incubated in the well for 5 hr in the presence of 1 $\mu\text{g}/\text{mL}$ GolgiPlug (BD), 1 $\mu\text{g}/\text{mL}$ GolgiStop (BD), 1,000 u/mL IL-2 (National Cancer Institute) and CD107a antibody. Following stimulation, the cells were stained for surface markers in order to identify NK cells, and intracellular IFN- γ .

Quantitative RT-PCR

Total RNA was isolated RNAeasy kit (QIAGEN) and reverse transcribed using iScript (Bio-Rad Laboratories) according to the manufacturer's protocol. Q-PCR was performed on a CFX96 thermocycler (Bio-Rad Laboratories) using SSO-Fast EvaGreen Supermix (Bio-Rad Laboratories). *Rpl19* and *Actin* were used as references.

Type I IFN Bioassay

L929-ISRE IFN reporter cells have been previously described ([Sauer et al., 2011](#)). Briefly, L929-ISRE cells were pre-plated at 5×10^4 per well in flat bottom 96-well plates and incubated in medium for 5 hr. Following incubation, the cells were lysed in passive lysis buffer (Promega) for 5 min at room temperature. Cell lysates were incubated with firefly luciferase substrate, and luminescence was measured using SpectraMax Luminescence microplate reader (Molecular Devices).

QUANTIFICATION AND STATISTICAL ANALYSIS

Group sizes, number of replications, and explanation of the mean and error bars are provided in the figure legends. Statistical analysis was done using Prism software (GraphPad Prism software). Tumor growth experiments were analyzed with repeated-measures two-way ANOVA. Flow cytometry, QPCR, and Stimulation experiments were analyzed using two-tailed t tests or one-way ANOVA. p values less than 0.05 were considered significant. *p < 0.05, **p < 0.01, ***p < 0.001, ****p < 0.0001.

Clinical Data Analysis

All data were obtained from TCGA using the cbiportal website ([Cerami et al., 2012](#); [Gao et al., 2013a](#)). Correlation of gene expression was assessed using the Spearman coefficient. For survival analysis Kaplan Meier curves were plotted comparing the patient with the highest level (upper 33%) and lowest level of particular gene (lower 33%). The curves were compared using the log-rank test.

Immunity, Volume 49

Supplemental Information

Tumor-Derived cGAMP Triggers

a STING-Mediated Interferon Response

in Non-tumor Cells to Activate the NK Cell Response

Assaf Marcus, Amy J. Mao, Monisha Lensink-Vasan, LeeAnn Wang, Russell E. Vance, and David H. Raulet

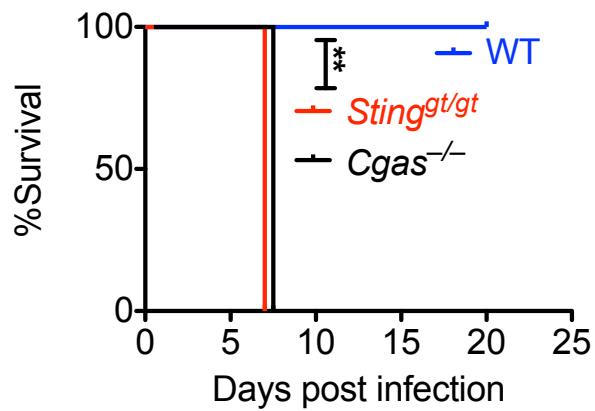


Figure S1. Validation of *Cgas^{-/-}* mice. Related to Figure 4.

WT, *Sting^{gt/gt}*, *Cgas^{-/-}* mice were infected with 10^7 PFU HSV-1 intravenously, and monitored for survival. Each group contained 4-6 mice. Statistical analysis was assessed using the log-rank test. Results are representative of two independent experiments.

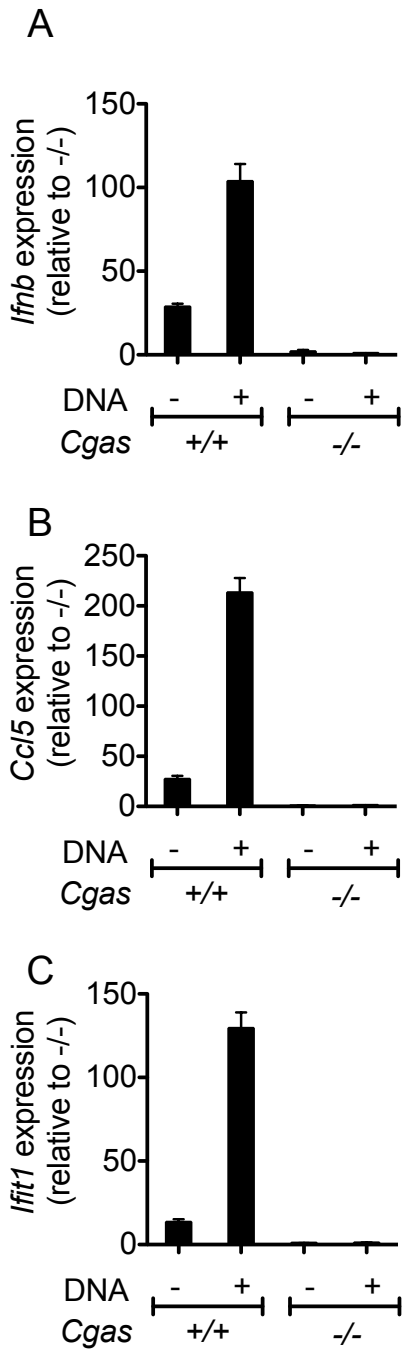


Figure S2. Validation of B16 $Cgas^{-/-}$ tumor cells. Related to Figure 6. B16- $Cgas^{+/+}$ and B16- $Cgas^{-/-}$ cells were transfected with HT-DNA, and assayed for *Ifnb*, *Ccl5* and *Ifit1* gene expression using Q-RT-PCR. Fold expression is shown relative to $Cgas^{-/-}$ cells. Results are representative of two to four independent experiments, and data consist of three technical replicates. Bars represent means \pm SEM.

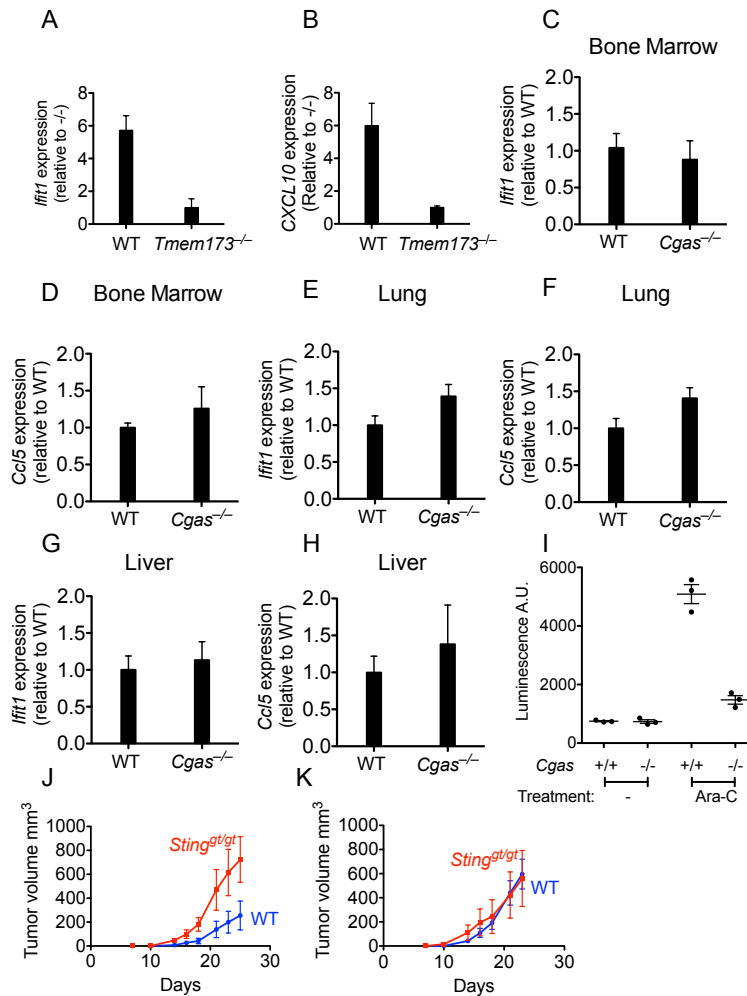


Figure S3. Activation of cGAS-STING in tumors *in vitro* and *in vivo*. Related to Figure 6.

(A-B) QRT-PCR analysis of *IFIT1* (A) and *CXCL10* (B) expression levels in THP1-*TMEM173*^{+/+}, and THP1-*TMEM173*^{-/-} tumor cells. Results are representative of two independent experiments, and data consist of three technical replicates. QRT-PCR analysis of *Ccl5* and *Ifit1* expression levels in Bone marrow (C-D), Lung (E-F), and Liver (G-H) cells isolated from WT or *Cgas*^{-/-} mice (I) B16-*Cgas*^{+/+} and B16-*Cgas*^{-/-} cells were incubated in media with or without 50 μM ARA-C, and after 48 hours secreted type I IFN was measured using an IFN bioassay. Tumor cells (10⁵) were injected s.c. into WT or *Sting*^{gt/gt} mice and tumor growth monitored as in Fig. 1 legend. Each group contained 4-6 mice, and results are representative of two independent experiments. Injected tumor cells were: B16-BL6-*Cgas*^{-/-} cells transduced with active (*Cgas*^{wt}, J), or inactive (*Cgas*^{mut}, K) CGAS expression vector. Bars represent means +/- SEM. Statistical analysis was done as in Fig. 1.

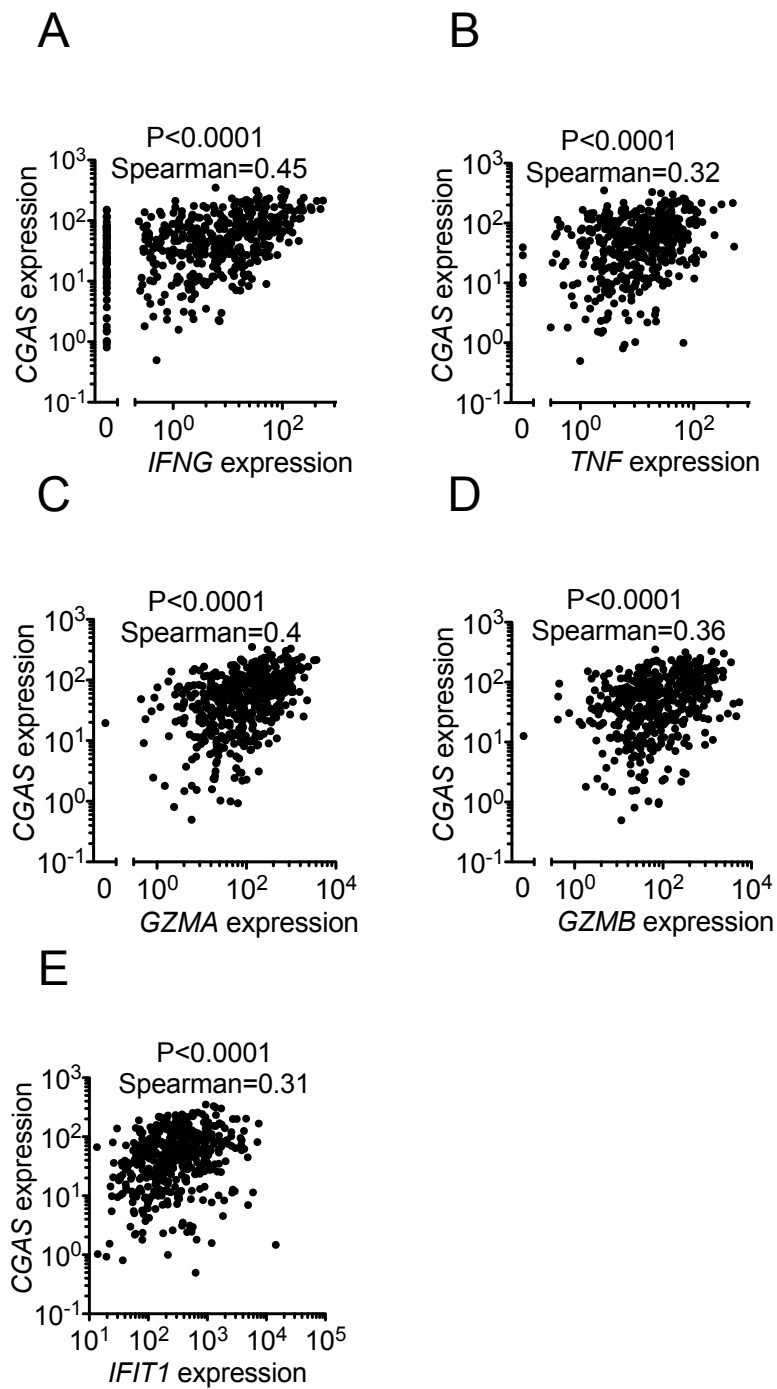


Figure S4. Correlation between cGAS expression and immune activation in melanoma patients. Related to Figure 7. Plots of expression of CGAS expression versus the immune activation markers *IFNG* (A), *TNF* (B), *GZMA* (C), *GZMB* (D), and *IFIT1* (E). All data were obtained from TCGA using the cBioportal website. Statistical correlation was assessed using the Spearman coefficient.

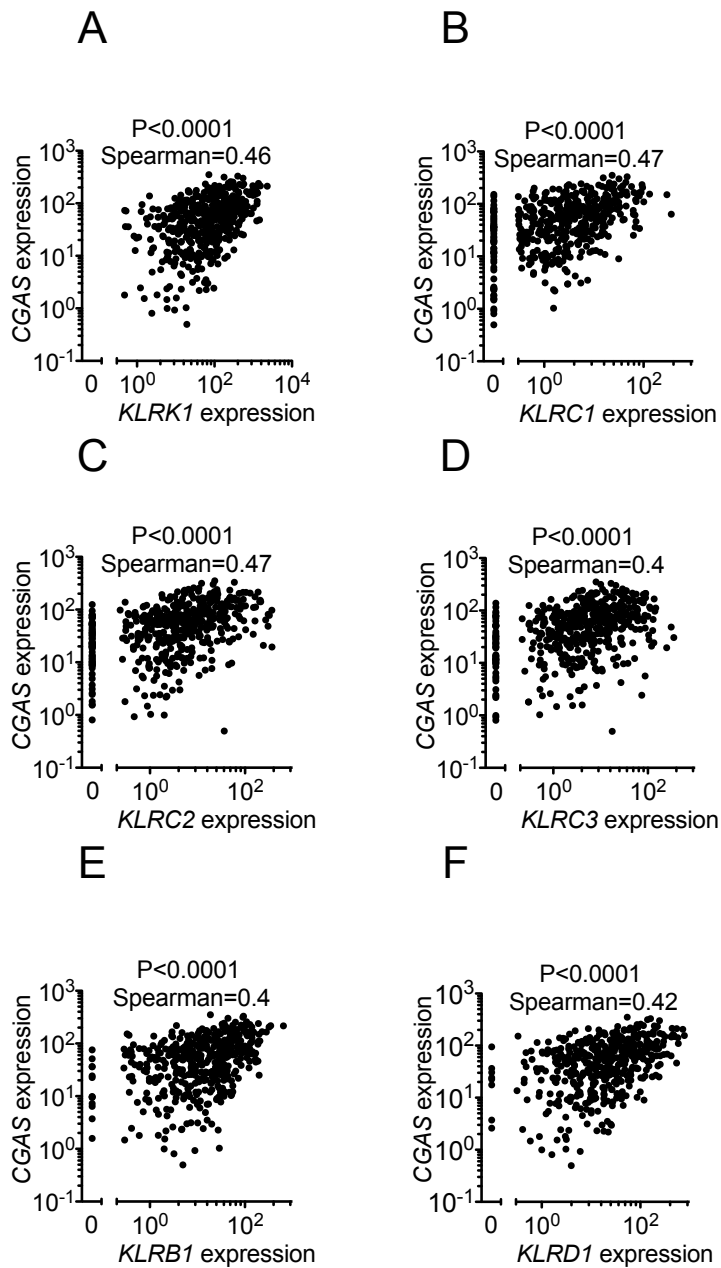


Figure S5. Correlation between cGAS expression and NK cell infiltration in melanoma patients. Related to Figure 7. Plots of expression of CGAS expression versus expression of the NK cell receptors *KLRK1* (A), *KLRC1* (B), *KLRC2* (C), *KLRC3* (D), *KLRB1* (E), and *KLRD1* (F). All data were obtained from TCGA using the cBioportal website. Statistical correlation was assessed using the Spearman coefficient.

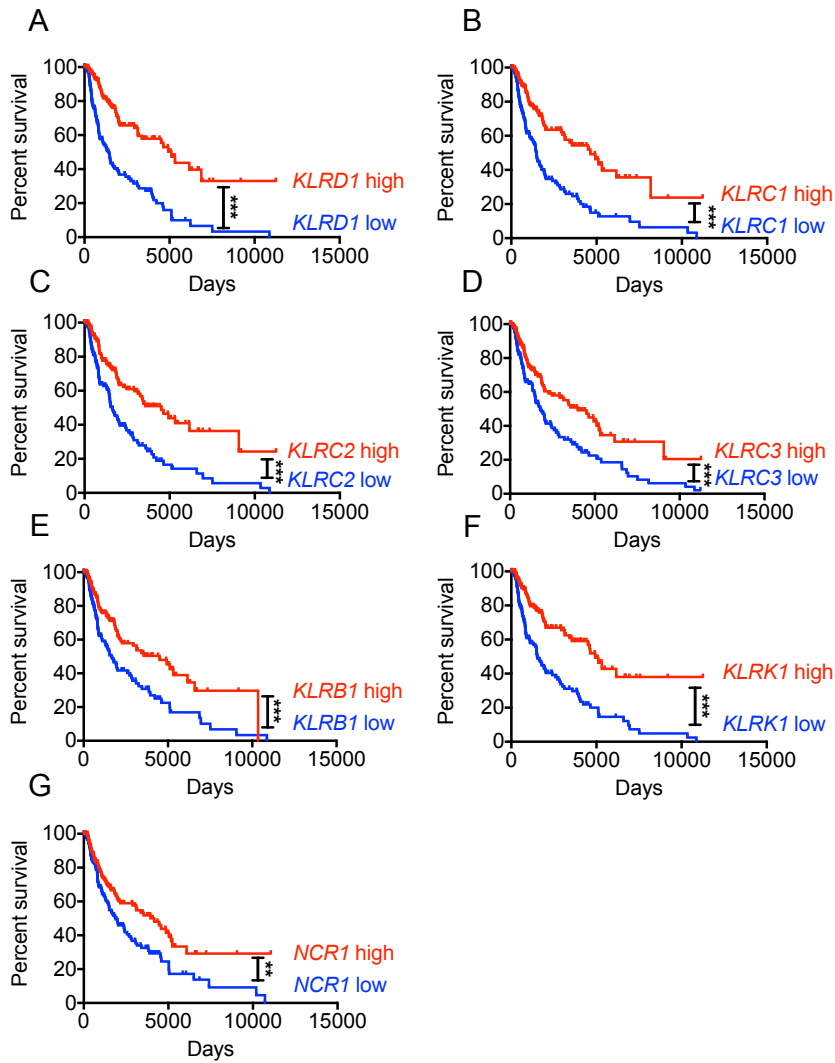


Figure S6. Correlation between NK cell infiltration and survival in melanoma patients. Related to Figure 7. Kaplan-Meier plots of melanoma patient survival. Patients were segmented by expression (highest and lowest thirds) of various NK cell receptors: *KLRD1* (A), *KLRC1* (B), *KLRC2* (C), *KLRC3* (D), *KLRB1* (E), *KLRK1* (F), and *NCR1* (G). Statistical analyses were performed using the log-rank test.

Table S1. List of forward and reverse primers used in qRT-PCR. Related to Star Methods

Target	Forward (F)	Reverse (R)
<i>mActin</i>	AGAGGGAAATCGTGCGTGAC	CAATAGTGATGACCTGGCCGT
<i>mRpl19</i>	GGCAGTACCCTTCCTCTTCC	AGCCTGTGACTGTCCATTCC
<i>mCcl5</i>	GCTGCTTTGCCTACCTCTCC	TCGAGTGACAAACACGACTGC
<i>mIfit1</i>	CTGAGATGTCACTTCACATGGAA	GTGCATCCCCAATGGGTTCT
<i>mIfnb</i>	TCCGAGCAGAGATCTTCAGGAA	TGCAACCACCACTCATTCTGAG
<i>hCXCL10</i>	CCTTATCTTTCTGACTCTAAGTGGC	ACGTGGACAAAATTGGCTTG
<i>hIFIT1</i>	ATCCACAAGACAGAATAGCCAG	CCAGACTATCCTTGACCTGATG